Report No. 101

DESIGN STUDY FOR THE MECHANICAL ATTACHMENT OF BRITTLE MATERIAL BLADES TO GAS TURBINE ROTORS

Contract Nonr 484(01)
Task Order NR 094-179

FINAL REPORT April 15, 1954

Prepared by: 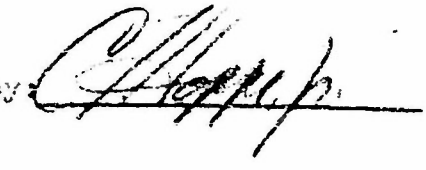

TABLE OF CONTENTS

TITLE PAGE	i
TABLE OF CONTENTS	ii
DISTRIBUTION LIST	iii
PREFACE	vii
SUMMARY	1
INTRODUCTION	1
THE PROBLEM	3
PROCEDURE	4
Stress Concentration	5
Preliminary Attachment Design Studies	7
Test Apparatus & Procedure	12
Test Results	16
Modification of Dovetail Design	18
Temperature Distribution	20
Cermet Material Data	22
Detail Analysis of Dovetail Attachment	23
Additional Considerations	26
CONCLUSIONS AND RECOMMENDATIONS	27
REFERENCES	29
TABLES	30-33
FIGURES	34-55

DISTRIBUTION LIST FOR
Unclassified Technical and Final Reports
Issued under Contract Nonr 484(01), NR 094-179
(Revised 5 November 1953)

Chief of Naval Research Department of the Navy Washington 25, D.C. Attn: Code 429	2
Commanding Officer Office of Naval Research Branch Office 346 Broadway New York 13, New York	1
Commanding Officer Office of Naval Research Branch Office Tenth Floor, The John Crerar Library Bldg. 86 East Randolph Street Chicago 1, Illinois	1
Commanding Officer Office of Naval Research Branch Office 1030 E Green Street Pasadena 1, California	2
Commanding Officer Office of Naval Research Branch Office 1000 Geary Street San Francisco 9, California	1
Commanding Officer Office of Naval Research Navy #100 Fleet Post Office New York,New York	2
Chief, Bureau of Aeronautics Department of the Navy Washington 25, D. C. Attn: PP-22 TD-4 AE-4	 2 1 1
Chief, Bureau of Ships Department of the Navy Washington 25, D. C. Attn: Code 541 Code 343	 1 1

Director
Naval Research Laboratory
Washington 25, D. C.
Attn: Technical Information Officer 6

Office of Technical Services
Department of Commerce
Washington 25, D. C. 1

Armed Services Technical Information Agency
Documents Service Center
Knott Building
Dayton 2, Ohio 5

Commanding General
Wright Air Development Center
Wright-Patterson Air Force Base
Dayton, Ohio
Attn: WCR 1
WCN 1
WCLPG5 1

Director National Advisory Committee for Aeronautics
1724 F Street, N. W.
Washingtin 25, D. C.
Attn: Division Research Information 2

Superintendent
U. S. Naval Post-Graduate School
Monterey, California 1

Central Intelligence Agency
2430 E Street, N. W.
Washington 25, D. C.
Attn: Liaison Division OCD 1

Office of Ordnance Research
U.S. Army, Box CM, Duke Station
Durham, North Carolina 1

Commanding General
Air Research and Development Command
P. O. Box 1395
Baltimore 3, Maryland 2

Library Branch
Office of the Secretary of Defense (R&D)
Room 3E 1065
The Pentagon
Washington 25, D. C.
Attn: Mr. C. R. Flagg 2 1

Committee on Aeronautics
Office of the Secretary of Defense (R&D)
Room 3E-133, The Pentagon
Washington 25, D. C. 1

Batelle Memorial Institute
505 King Avenue
Columbus 1, Ohio
Attn: Dr. B. D. Thomas 1

Marquardt Aircraft Company
7801 Hayvanhurst Avenue
Van Nuys, California
Attn: Mr. R. E. Marquardt 1

Pratt & Whitney Aircraft Division
United Aircraft Corporation
E. Hartford, Conn. 1

Fairchild Engine and Airplane Corporation
Fairchild Engine Division
Farmingdale, L.I., New York
Attn: Mr. T. F.Hammen, Jr. 1

McDonnell Aircraft Corporation
P.O. Box 516
St. Louis 3, Missouri
Attn: Dr. B. G. Bromberg 1

Reaction Motors, Inc.
Stickle Avenue and Elm Street
Rockaway, New Jersey
Attn: Mrs. Margaret Becker, Librarian 1

Wright Aeronautical Corporation
Wood-Ridge, New Jersey
Attn: Sales Department (Government) 1

Boeing Airplane Company
Seattle 14, Washington
Attn: Mr. R. H. Nelson 1

Lycoming Division
Avco Mfg. Corp.
Williamsport, Pa. 1

Westinghouse Electric Corp.
Aviation Gas Turbine Division
Essington, Pa. 1

Allison Division
General Motors Corp.
Indianapolis 6, Indiana 1

AiRcsearch Mfg. Co.
Los Angeles 45, Calif. 1

Solar Aircraft Co.
San Diego, California 1

Research Department
United Aircraft Corp.
East Hartford 8, Conn. 1

American Electro Metal Corp.
320 Yonkers Avenue
Yonkers 2, N. Y. 1

Continental Aviation and Engineering Corp.
1500 Algonquin Avenue
Detroit 14,Michigan
Attn: Mr. Whitney Collins 1

Thompson Products, Inc.
Staff Research & Development
2196 Clarkwood
Cleveland 3, Ohio 1

Kennametal, Inc.
Latrobe, Pa.
Attn: Mr. J. C. Redmond 1

General Electric Company
Aviation Gas Turbine Division
Evendale, Ohio 1

General Electric Company
Turbine Division
Schnectday, New York 1

Aerojet-General Corporation
Azusa, California
Attn: Librarian 1

Chief of Naval Operations
Department of the Navy
Washington 25, D. C.
Attn: Op 51 1

Chief, Bureau of Ordnance
Department of the Navy
Washington 25, D. C.
Attn: RE 3a 1

National Advisory Committee for
Aeronautics
Lewis Flight Propulsion Laboratory
Cleveland, Ohio 1

PREFACE

This Document is the final report of the research activities conducted in compliance with the Office of Naval Research Contract Nonr-484(01), Task Order NR 094-179.

This task was entitled "Design Studies for the Application of Brittle Materials to Gas Turbines". The scope of the task was clarified in subsequent correspondence and discussions which emphasized that the design studies (and test work as required) should seek a solution to the problems associated with the attachment of non-ductile material turbine blades to a ductile rotor disk. The studies were based upon dimensional and operating data for a small auxiliary gas turbine as approved by the Office of Naval Research.

We wish to acknowledge the cooperation and assistance of the many industrial organizations and government agencies which have been so helpful in the conduct of this research.

DESIGN STUDY FOR THE MECHANICAL ATTACHMENT OF BRITTLE MATERIAL BLADES TO GAS TURBINE ROTORS

SUMMARY

A design study was conducted resulting in the design of a mechanical attachment for a brittle turbine blade to a ductile rotor disk and an analytical determination of the maximum effective gas temperature and service life of the attachment in a specific application. Included are brief analyses of the required assembly clearances to provide for dissimilar thermal expansion rates, the effect of rotor rim cooling on the attachment problem, and a detailed description of the methods used for the readers' reference. Tests were conducted to determine a suitable ductile material insert and to qualitatively compare designs. Analysis of the final design when applied to a small auxiliary gas turbine indicates that, with an uncooled rotor, at an effective gas temperature of 1820°F. the attachment life is 100 hours and blade life is 1000 hours. With a cooled rotor, at a temperature of 1920° F. the attachment life exceeds 1000 hours while the blade life is 100 hours.. Figures are based upon calculated temperature distributions and upon available stress-rupture data for several cermet materials since no high temperature life tests were conducted. It is concluded that the attachment design is satisfactory for the application and would permit increased turbine operating temperatures insofar as the blade and attachment strangths are concerned. Considerations which may limit the use of brittle blades are noted as are the assumptions for and limitations of the analyses presented.

INTRODUCTION

In the search for improved performance, the gas turbine designer looks for solutions to a great number of problems. While they may disagree as to the relative importance of the various problems and in the best approach to their solution, all will agree that substantial increases in power without sacrificing efficiency can be obtained by increasing turbine operating temperatures. Present designs are limited by the ability of the available highly-alloyed materials to withstand higher temperatures. This is generally true of all the hot parts in the engine such as combustion chamber liners, nozzle box and vanes, turbine rotor and blades, and the exhaust system.

It is expected that solutions to the oxidation and thermal shock problems involved will be found in metallurgical advances, development of temperature resistant coatings, and improved cooling methods, etc. Research and development toward the solution of these problems is progressing in each of these fields and shows considerable promise. The problems of oxidation and thermal shock resistance are common to all of the above components and are the major obstacles in the path to higher temperatures for all of the components except the turbine rotor and blades which are subjected to high stress as well as high temperature.

Rotor disks are subjected to varying biaxial stresses due to centrifugal loads and temperature distribution. Elastic deformation and, in some cases, plastic flow of the disk material results in reduced maximum stresses and more uniform stress distribution. Thus, ductility is essential to thedesign of gas turbine rotor disks and to the efficient use of disk materials. Therefore, as far as the turbine rotor is concerned, the increase of operating temperatures depends largely upon the development of cooling methods to limit the disk material temperature and/or the development of new ductile materials capable of withstanding higher temperatures.

Turbine blade cooling can reduce blade material temperature substantially below the gas temperature. Considerable progress has been made in developing cooling methods and blade designs to accomplish this and thus to increase gas temperatures. In addition, new materials have been developed which exhibit satisfactory oxidation and thermal shock resistance for use in turbine blades at higher temperatures. However, the ductile materials lack sufficient stress-rupture strength for even small temperature increases, and the materials which promise relatively large temperature changes are primarily non-metallic and present difficult design problems in their attachment to metallic rotor disks. The attachment problems are due to the dissimilar physical characteristics of the two materials being joined, such as coefficient of thermal expansion, and to the fact that the non-metallic materials are extremely brittle.

The design studies reported herein are directed at the problem of achieving a satisfactory mechanical attachment between a brittle turbine blade and a ductile rotor disk, and an analytical determination of the maximum effective gas temperature and service life of this attachment design in a specific application. Included in the study are brief analyses of the required assembly clearances to provide for dissimilar thermal expansion rates, the effect of rotor rim cooling on the attachment problem, and a detailed description

of the methods used for the readers' reference. While it is recognized that brittle materials lack impact resistance and that this shortcoming could seriously reduce the predicted service life of brittle turbine blades, this problem is considered to be associated with the selection of material rather than the design of an attachment. Therefore, no consideration is given to impact resistance in this report.

It should be noted here that the results of most of the above research and development will make a valuable contribution to the conservation of strategic materials. The scarce alloying elements are used primarily for improved properties at elevated temperatures. The development of temperature-resistant coatings, new cooling methods, and cermet materials will undoubtedly permit the use of less strategic alloys at present temperatures in many applications where temperature increases are either not desirable or not feasible until satisfactory solutions to the remaining problems are found.

THE PROBLEM

The primary load involved in attaching a blade to a turbine disk is tension caused by the centrifugal force of the rotating blade itself. The bending load resulting from the gas forces is small relative to the centrifugal loads. It can be counteracted by offsetting the blade centroidal axis from the radial line through the neutral axis of the attachment by an amount which equalizes the resulting moment due to centrifugal load and the moment due to gas load. Vibration is a serious problem if the natural frequency of the blade is less than six to eight times the rotational speed of the rotor.

The design of a mechanical attachment for such a blade involves one or more notches and a like number of lands or load-bearing surfaces. The load is transferred from the blade base to the rotor segment on the disk periphery either by mating the shape of the contacting surfaces in the two components or through a pin which mates with notches in each of the bodies. In either case the area available to resist the tension load is reduced adjacent to the load-bearing lands. The maximum tensile stresses occur at such points. In order to keep bearing-land area to a minimum, blade attachments are run with high bearing stresses. This demands that the bearing contact surfaces mate nearly perfectly under load in order to insure a uniform load distribution and prevent local failure.

For ductile material blades these problems have been

solved by using various modification of the "fir-tree" or "pine-tree" attachment. Due to the ability of the material to deform and distribute load, a relatively small load is taken on eachone of the multiple load-bearing lands. The lands and, therefore, the notches can be small, and relatively large cross-sectional areas are available to resist the tension load. Reasonable production tolerances can be allowed in fabricating the attachment because of the material's ability to deform and achieve a perfect fit under load.

Blades of a brittle material, on the other hand, will not deform under load and aresubject to high stress concentrations in tension due to notches or changes in section and in bearing due to lack of fit or surface conditions which result in line-contact or point-contact rather than in a uniform load distribution over the bearing area. It is apparent that a satisfactory design for the attachment of brittle material blades to a gas turbine disk must minimize the concentration of stress in tension and incorporate some means of insuring uniform bearing load distribution. These are the two major problems to be solved.

In addition to the above requirements, a satisfactory attachment design must not allow the brittle material blade base to be subjected to large bearing or crushing loads which can result fromthe combined effects of rotor plastic flow and the different rates of thermal expansion of the two materials. Also, cognizance must be taken of the fact that the the thermal conductivity of the cermet materials considered is greater than that of current blade alloys and will permit more heat flow into the rotor rim. A satisfactory design for use with current rotor disk materials must include provisions for limiting the temperature distribution in the disk if higher operating temperatures are to be obtained. Vibration is not considered to be a serious problem with brittle material blades since the natural frequency of such a bladeis in the order of twice the frequency of itsmetal alloy counterpart.

PROCEDURE

The procedure followed in conducting the design study was primarily an analytic one. Experimental work in the form of strength testing was used as a design tool only in those instances where problems were intangible and not amenable to analytic solution. The procedure is described in the approximate order in which the study work was conducted.

A non-dimensional design chart was prepared showing the effects of notch-radius and notch-depth upon the stress

concentration factor to be applied to the tensile stress in the neck of a notched member in tension. This chart makes it possible to select the proportions of a blade base such that the stress concentration factor will be minimum.

Comparative strength tests were conducted to determine a satisfactory means of obtaining a reasonably uniform load distribution on a load-bearing surface. Brittle material specimens were loaded in a centrifugal test apparatus in order to simulate actual load conditions.

Several attachment designs were analyzed and compared. The designs were consistant in that the rotor segment strength was held constant as was the space envelope containing the blade base and rotor segment. Comparative strength tests were conducted to establish the merit of any design having features which were expected to be improvements the extent of which were not determinable by analysis.

The design considered to be superior was selected and subjected to a complete analysis to determine the maximum temperature vs. life expectancy when used in a small auxiliary gas turbine rotor. Temperature distributions were calculated at several effective gas temperatures for both an uncooled rotor and one with rim-cooling fins. The available stress-rupture data for several cermet compositions and one currently-used disk alloy were used in determining the optimum attachment configuration and the maximum temperature capability for several service life expectancies.

A rotor disk profile was designed to incorporate the necessary changes due to reduced blade loading and increased temperature gradient. Several suggested designs for methods of retaining the blades in the disk were prepared, and a brief analysis was made to determine the assembly clearances required to insure that the blades would not be overconstrained at any time during the operating cycle.

Stress Concentration

The non-dimensional design chart of Figure 1 shows the effect of notch-radius and notch-depth upon the concentration of tensile stress in the blade base. The dimensional nomenclature is shown in Figure 2. The family of curves are obtained from the data of references 1 and 2. The loading condition of the references is pure tension through the notched area while a turbine blade attachment is loaded in the notch with accompanying large bearing loads. The determination of the effect of notch-loading involves a test program which is beyond the scope of this study. Consequently, the bearing limit curve of Figure 1 is taken from reference 3 which reports the results of such a test program.

Notch proportions above the limit curve result in bearing failures while those below result in tension failures.

The limit curve applies strictly to methyl methacrylate plastic specimens loaded in a universal testing machine equipped with a polariscope to preclude eccentric or variable loading. The curve is assumed to be a maximum for brittle material turbine blade attachments for the following reasons:

(1) The plastic material shows somewhat more ductility than ceramics or cermets.

(2) Bearing loads will not be uniform in turbine blade attachments due to the mass distribution of the cambered airfoil.

(3) Load eccentricity between bearing lands is more possible with turbine blades due to fabrication tolerances.

(4) Centrifugal loading results in bearing loads on the lands which are greater than the tension load in the neck of the blade base due to the mass below the neck.

The curve as shown was used for design purposes since little else is known about the characteristics of notch loading and such factors as the ratio of bearing stress to tensile stress of different materials and the inherent variations of experimental data might favor the use of somewhat higher bearing load limitations. However, consideration is given to items (2), (3), and (4) above in accounting for unexpected bearing failures during test, and in improving attachment designs which otherwise appear to warrant such development.

It is apparent from Figure 1 that the optimum proportions of a blade base for maximum load factor with adequate bearing strength are approximately as follows:

r/D_b = 0.4 to 0.5
d_b/D_b = 0.65 to 0.70
r/h = 2.3 to 2.7

These proportions result in a maximum load factor of approximately 0.462 which indicates that the blade neck will carry 46 percent of the tensile loadthat the base would carry without notches.

It should be noted that an attachment configuration with the maximum load factor is not necessarily the optimum for a particular type of design since the optimum design requirement is minimum blade neck stress at the total centrifugal load of both the blade and base while maintaining adequate strength in the rotor rim segment. This is shown by the equation for blade neck stress.

$$\sigma_{t,\,b} = \frac{P_b}{(d_b/D_b K_f)\, D_b t} \qquad (1)$$

Where P_b equals centrifugal load due to the blade and the portion of the base above the neck. The base thickness (t) is considered a constant throughout the study since it is determined by the root chord of the blade. Since P_b and D_b are affected by several factors including the parameters which determine the load factor $(d_b/D_b K_f)$, it is evident that a minimum stress may occur with other than a maximum load factor. The section of this report entitled "Preliminary Attachment Design Studies" deals more fully with this subject.

Preliminary Attachment Design Studies

In order to make a preliminary comparison of several different types of attachment designs, it isnecessary to establish a standard set of operating conditions. The conditions assumed are for the small auxiliary gas turbine at its design speed of 36,000 RPM. These are 55 blades per wheel on a diameter at the root platform of 5.11 inches. The centrifugal load at the blade root platform is 980 pounds based upon a cermet density of 0.21 pounds per cubic inch.

For each type of attachment the critical rotor rim stress is held constant at approximately 36,000 p.s.i. which is equivalent to the 100 hour stress-rupture strength of Timken 16-25-6 alloy at 1270° F. This value is arbitrarily chosen as representative of a reasonable maximum value for this material. Each attachment configuration is varied until a minimum blade neck stress including stress concentration factor is obtained. Comparisons are then made on the basis of blade neck stress. The configuration having the lowest stress is considered to be the best design.

The attachment types investigated are shown in Figure 3. Several other types were considered but not subjected to preliminary analysis because of obvious lack of advantage in comparison with those reported here. Conventional and modified fir-tree bases were rejected because of the difficulty in obtaining generous radii and the extreme

precision of fabrication required for uniform loading between bearing lands. Multiple round-pin type attachments were rejected for the same reasons. All types which require a split turbine disk were rejected because of the variations in temperature, stress, and deformation between the two disks during a normal operating cycle.

Blade neck stress is calculated using Equation (1). The load, P_b, is computed for each configuration at the design conditions using the following equation.

$$P_b = 980 + 36{,}780\ \rho_c\ V_c\ \bar{r} \quad \text{(lb)} \qquad (2)$$

where:

ρ_c = density of cermet (lb/cu.in.)(0.21 for study)

V_c = volume of cermet base above neck (cu. in.)

$\bar{r}$ = mean radius to centroid of V_c (in.)

The load factor, (d_b/D_bK_f), is taken from Figure 1. The maximum width, D_b, is determined by, (1) the requirement for 55 blades or, (2) the optimum blade base proportions to give minimum stress. The thickness, t, is held constant at 0.663 inch throughout the study.

Dovetail Attachment

The dovetail type of attachment is a simple mechanical attachment which can be easily fabricated, incorporates large radii, and involves no pins or auxiliary attachments other than a means of retaining the blade in the disk. It can be designed to attain the maximum load factor shown on Figure 1 ($d_b/D_bK_f = 0.462$). In this optimum configuration the stress in the blade neck is approximately 21,700 p.s.i. with a rotor segment stress of 36,000 p.s.i. The shear stresses across the lands of both the blade base and the rotor segment have adequate margins of safety. Sufficient space is available to provide for variations of the attachment loads, stresses, and design details without compromising the essential features of the design or seriously affecting the size and weight of the rotor disk.

This attachment design when used in conjunction with a thin, ductile metal insert is judged to be superior to the other types investigated. It is subjected to a thorough analysis later in this report in an attempt to arrive at an optimum attachment for a given application in terms of operating temperature and service life.

Pin-in-Longitudinal Shear Attachment

Round pin type attachments are attractive because they are easy to fabricate and assemble in mass production and because the attaching pins may be made of a soft, ductile material to distribute the bearing loads evenly across the lands of the cermet blade base. It is possible to obtain a configuration with a maximum load factor. However, the accompanying total width, D_b, is very small and the corresponding rupture strength is relatively low. The maximum strength configuration occurs with a notch radius to notch depth ratio of approximately unity ($r/h = 1.0$). The minimum blade neck stress with a rotor segment stress of 36,000 p.s.i. is approximately 26,000 p.s.i. The attaching pins are only slightly larger than 1/32-inch in diameter and must carry a shear stress of over 27,000 p.s.i. It is likely that a ductile material insert would be required to distribute the bearing loads since any material capable of this shear stress at elevated temperatures would be quite hard. Shear strength is assumed to be 70% of the tensile stress-rupture strength for all materials since actual shear strength data are not available.

This attachment is not as strong as the dovetail, requires more parts since both pins and ductile inserts are needed for load distribution, and is very sensitive to changes in design. That is, the optimum proportions do not remain the same as the ratio of blade neck width to rotor segment width are varied in order to obtain the optimum attachment for a given application. It is concluded that the basic weakness of this type is that both the blade base and rotor segment must be reduced in strength in order to provide space for the attaching pins. Two other attachment types are the result of attempting to avoid this weakness in the design of a pin-type attachment.

Pin-in-Sectional Shear Attachment

This attachment design permits the blade base width to be increased by transferring the load from the blades to the rotor disk through leading-and trailing-edge flanges rather than through rotor segments. This configuration allows the blade base and attaching pins to occupy the entire perimeter of the rotor disk. Assembly of the blades to the wheel should be simple and the pins can be retained by peening the ends as is currently done with alloy blades.

Investigation of this design discloses that the major problem is to provide sufficient shear strength in the pins.

In order to realize the inherent advantages of this type of attachment, the pin area must be kept reasonably small. The high allowable shear stress required is furnished only by alloy materials with high cobalt and/or nickel content. Round pins are desirable to permit fabrication of the pin retaining holes in the wheel rim by drilling and reaming rather than by broaching. However, round pins of sufficient area reduce the blade base neck width and thus the load factor below practical values. A high load factor near the maximum can be obtained by using non-circular pins. A design of this type is shown in Figure 3. The blade neck stress is approximately 21,000 p.s.i. and the pin shear stress is approximately 39,000 p.s.i. It is apparent that this attachment is much larger and deeper than the other types and incorporates a large odd-shaped pin with a small edge distance to resist bearing loads at the rim of the rotor disk.

While the calculated stress conditions appear to be superior, several considerations make the realization of these conditions quite doubtful, and further, if realized, whether the relatively small stress advantage over the dovetail type would exceed the disadvantages. These considerations are listed below.

(1) The wheel rim flanges extend up to the top of the blade platform and are subjected to the full inlet gas temperature. The resulting wheel rim temperatures will be higher.

(2) The edge distance in bearing is small, and any increase will increase the operating loads and reduce the load-resisting areas. Combined with par.(1) above, this design might prove inadequate to realize the stress conditions shown.

(3) The larger blade load andthe load from the flanges at the wheel rim result in rotor disk loads which are greater than for the other types. Therefore, the rotor will be larger and heavier.

(4) The retaining pins are operating atvery high shear stresses even when thebest of the super-alloys at reasonably moderate temperatures are considered. It is difficult to modify the design to reduce these stresses without nullifying the blade base neck stress advantage.

(5) One of the pins contains approximately the same amount of critical material as an entire conventional blade for this turbine made of the same alloy.

(6) The wheel rim attachment holes are very difficult to fabricate, as are the pins themselves to a lesser extent.

Pin-in-Compression Attachment

This type of attachment allows the blade base and the rotor segment to interlock with each other such that the pin size does not limit the blade neck width as in the pin-in-longitudinal shear type. With round pins it is not as easy to fabricate as the dovetail or pin-in-longitudinal shear types, but with non-circular pins it is perhaps the simplest of all types. Since the pin is in compression it can be made of relatively soft material and require no additional ductile material insert to distribute the bearing loads.

Using round pins, somewhat lower stresses are developed in the blade neck than with the pin-in-longitudinal shear attachment. The stress level is still inferior to the dovetail configuration. However, with non-circular pins, as shown in Figure 3, the maximum load factor can be developed and the stress level is comparable to that of the dovetail type. It is slightly inferior because the loads are greater due to the greater depth of attachment required to furnish adequate shear area in the outer portion of the rotor segment since the pin occupies space which is used to resist shear load in the dovetail design. This configuration is judged to be a close second to the dovetail since strength is about equal and ease of fabrication and assembly is about the same except for the non-circular pins used with the interlocking design.

In summary of the preliminary attachment design studies, the evaluations of the various types of attachment designs fall in the following order of superiority.

(1) Dovetail
(2) Pin-in-Compression (non-circular pin)
(3) Pin-in-Sectional Shear (non-circular pin)
(4) Pin-in-Longitudinal Shear
(5) Pin-in-Compression (round pin)
(6) Pin-in-Sectional Shear (round pin)

As a result of this evaluation, the Dovetail attachment is subjected to a detailed design analysis for various operating conditions and using several representative cermet blade materials in a later section of this report.

Test Apparatus and Procedure

Tests are necessary to determine an effective means of preventing attachment failure due to local concentrations of bearing stress on the blade base bearing lands and to evaluate design modifications whose effects cannot be determined satisfactorily by analysis. These objectives can be achieved by a test program based upon the comparison of one design or technique with another in order to select the better of the two, just as well as, by a more elaborate program which would yield absolute values for each possibility. Absolute magnitudes are analytically determined in this investigation, and checking their validity requires full-scale engine testing. It is required, however, that all aspects of the test program be consistent to insure valid comparisons, be capable of simulating the significant material properties and loading conditions, and be economical. Consequently, a centrifugal test apparatus of simple design is used in order to simulate actual turbine loading conditions. The tests are conducted at room temperature since the cermets under consideration are most brittle at low temperatures. The specimens are made of an inexpensive but very brittle ceramic material. Great care is exercised to insure consistency between groups of specimens both in their fabrication and in their testing.

Test Equipment

The test installation is shown in Figure 4 and consists of a spin chamber with a vacuum-sealed removable top enclosed in a concrete and steel protective barricade, an air-turbine drive system, a vacuum system, a mechanical hoisting system, and appropriate instrumentation. The spin chamber consists of a 24 inch diameter steel cylindrical shell 3/8 inch thick permanently sealed at the bottom with a one inch steel plate, and covered at the top with a 1-1/2 inch steel plate which seals by dead weight and external pressure against a neoprene seal mounted in a ring welded to the top of the shell. The top includes two small plexiglas observation windows and

mounting provisions for the drive system and electronic tachometer components. Inside the spin chamber 46 wooden blocks of special shape retained by steel rings at top and bottom absorb the impact of fragments from the ruptured specimens.

The air turbine drive system consists of an air turbine and bearing housing adapted from a Thompson Products Turbine Pump Assembly, an extension shaft and bearing housing which mounts to the spin chamber top, an emergency air brake system which mounts to the top of the turbine, and a muffler through which the turbine exhaust passes. The air is supplied by the plant compressed air system through a small reservoir to a pair of control valves, one each for turbine control and brake operation. The Thompson turbine is a radial flow type with 26 nozzles, and is designed for a much greater power output than required for this application. The plant air system is supplied by a 5HP compressor and it was found after some experimentation that with all but two of the turbine nozzles plugged, the turbine output was adequate and yet the plant air supply was not exhausted. The muffler is necessary to reduce the noise level of the exhaust and the turbine while in operation.

The vacuum system consists of a Kinney VSD-778 vacuum pump with oil separator and solenoid valve, a vacuum control valve, and air-line filter to protect the valve seats and pump from damage by ceramic dust, a vacuum release valve, and a vacuum gage. The vacuum pump has a rated capacity of 27 cubic feet per minute of free air and will pull a 10 micron Hg. vacuum in blank tests. However, the working vacuum in this installation is 29.5 inches of Hg. due primarily to air and water vapor drawn from the wooden blocks in the spin chamber.

The mechanical hoist system consists of a specially-designed three-legged sling which can be attached by hooks to either the spin chamber or its top and is connected at the upper end to a simple manila rope block and tackle arrangement and then to a heavy wooden frame.

The instrumentation consists of an air pressure gage, a vacuum gage, and a Hewlitt-Packard Model 505(a) Electronic Tachometer. The air pressure gage and vacuum gage are used only to determine the initial conditions for starting a test run, while the tachometer furnishes the test data to determine the relative strength of test specimens.

Test Specimens and Holders

The specimens subjected to test are shown in Figure 5. The Calibration and Standard specimens are used to check the physical properties of the material, the reproducibility of the test data and equipment, and the effect of test blade configuration on the apparent strength of the specimens. Data from tests of these specimens are also used to evaluate the relative merits of various types of ductile material inserts. The Dovetail and Skewed Dovetail specimens are used to determine the effects of the modifications incorporated in the skewed base configuration. This base is rotated 15 degrees with respect to the turbine axis and also incorporates flat attachment bearing lands which are tangent to the notch radii and subtend an included angle of 60 degrees. The effects of these changes are not readily determinable by analysis. The reasons for believing these modifications to be improvements are explained along with the methods used to determine the extent of the changes in the section of this report entitled "Modification of Dovetail Design".

Specimens are fabricated of feldspathic porcelain. Fabrication begins with a brass pattern of the specimen made sufficiently oversize to allow for shrinkage. Patterns are made in two pieces so that each blade pattern can be attached to each of the four base patterns. This precludes the necessity of duplicating the complex blade pattern for eachbase design.

Plaster of Paris molds are made from the patterns, and a low-pressure casting technique is used to cast the blended feldspathic porcelain raw materials. All specimens are fabricated from a single batch of blended materials to insure consistent composition. The casting is dried in the mold for approximately 24 hours and air-dried for at least 48 hours after removal from the mold. The specimens are then fired at Cone 12 for 24 hours. Extreme care is exercised to insure that the firing conditions for each batch of specimens are essentially identical. This procedure results in very consistent dimensions from specimen to specimen with maximum differences amounting to plus or minus .005 inch.

After firing, the specimens are inspected by X-ray and by penetrant dye for internal and external defects. Rejections average about 10% for all batches except the early ones during which the casting technique was being developed. After inspection, the specimen base is ground to the final contour to an accuracy of plus or minus .001 inch. The surface finish is very smooth. A silicon

carbide grinding wheel, grade G or H, 80 or 120 grit, is used. The work is flooded with coolant during the grinding operation. Grinding fixtures are surface ground blocks with a hole to receive the blade portion of the specimen and three locating points for the root platform surface. The specimen is inserted in the hole and lightly clamped with the base portion extending out of the fixture and the hole is filled with molten sulphur which solidifies to retain the specimen and then is melted to release the specimen after grinding. The final operation is to grind the tip of the blade to finish length using the test holder as a grinding fixture. Final inspection includes weighing each specimen; all agree within plus or minus 4% of the mean weight within a group of comparable specimens.

Specimen holders are made using standard machine shop techniques. The attachment contour is formed using a special end mill ground to shape using the same wheel used to grind the specimen base. This wheel is dressed after each complete operation using a ten-times scale template and a diamond-point dressing tool. The holders used in the initial tests are made of 24ST aluminum alloy rolled plate and SAE 1018 cold rolled steel to determine the effect of holder ductility and hardness. Cold rolled steel holders are used in all subsequent tests to more nearly approximate turbine materials. Counterweights are made of the same material as the holders and are dynamic duplicates of the specimen-holder combinations.

Test Procedure

In all except Run 1, one specimen and its corresponding counterweight are installed on the wheel as shown in Figure 4(c). The specimen is held loosely in the holder by a set-screw to prevent its falling out during handling and initial acceleration of the test rig. In most of the runs a ductile material insert is placed between the mating surfaces of the specimen and holder. The assembled wheel is then checked for static balance. The entire rotating assembly less specimen, holder, and counterweight had previously been balanced statically and dynamically at all speeds up to 25,000 RPM.

The absolute pressure in the spin chamber is reduced to less than one inch of mercury, and the specimen is rotated up to the soaking speed and held at that speed for approximately one minute to insure thatthe speciman does not move inthe holder and that the mating surfaces

are contacting each other properly. Rotation is stopped and a visual inspection is made through the inspection windows to check the above conditions. The speed is then increased as uniformly as possible until failure occurs. The loading rates are very low in terms of psi/second. The speed of the test rig is controlled manually, but the rate of speed increase is coordinated with vocal check points from a stop-watch in order to keep the loading rate as consistent as possible. The failure speed is recorded and the specimen is removed and examined to determine the location and type of failure.

Test Results

The test data is given in Table 1. Runs 1 through 7 represent the familiarization phase to get acquainted with the equipment and the ceramic material. These specimens are the only ones furnished by the first supplier who cancelled further participation in this program due to a change in the nature of his business. The first tests indicate that holder ductility has a pronounced effect upon the apparent strength of the specimens. The specimens tested in 24ST aluminum alloy holders average 47% greater strength at fracture than those tested in cold rolled steel holders. The location of the first fracture was in doubt during the first five runs because of the large number of fractures evident after each test. The nature of this fragmentation of the specimens is shown in Figure 6. Runs 6 and 7 include a special 24ST retainer assembly to furnish additional support to the base but not the blade and to retain the base fragments. The specimen after fracture is shown in Figure 7. There are three small fragments at the mating surface just above the arc-shaped neck fracture which indicate that the initial failure is due to bearing stress at that point. The 25% increase in fracture load corroborates this conclusion. The fracture of the blade at the root is probably explained by the phenomenon of double fracture in tensile testing of brittle materials. An analysis by the method given in reference 4 indicates that a secondary fracture at the blade root is probable following a primary fracture at the base neck.

Selection of satisfactory Ductile Insert.

Runs 8 through 28 are intended to determine a satisfactory ductile insert and to determine the effect of specimen blade shape on the apparent strength of the specimens. Ductile materials considered for use as inserts are .005 and .010 inch solid copper sheet, .010 inch brass

wire screen, .005 in. electrolytic copper plating, and .005 inch nickel-plated, perforated copper screen. There is little difference between the two gages of solid copper sheet. The average rupture speed for all standard and calibration specimens tested with these inserts is 10,170 RPM. The average for the brass screen is 10,950 RPM. The copper plating does not adhere to the ceramic material and was dropped from consideration after a single test. The average rupture speed for all calibration and standard specimens tested with perforated screen inserts is 11,000 RPM. The perforated screen has a negligible strength advantage over the woven brass screen but it has two other advantages which result in its recommendation. It is easier to form to the shape of the attachment contour and its resistance to high temperature and to the oxidizing atmosphere of gas turbine operation should be decidedly superior.

The calibration specimens with circular blades demonstrate only 8% greater strength than the standard specimens with airfoil shaped blades. However, the airfoil-shaped blades are not as difficult to fabricate as had at first been anticipated and thus there is no advantage to be gained by using the simpler, less representative circular blade. The remainder of the tests are conducted using airfoil blade specimens and perforated screen for inserts with one exception.

Dovetail vs. Skewed Dovetail Specimens

The objective in modifying the dovetail base to the skewed configuration with flat bearing lands is to reduce local bearing load concentrations by distributing the bearing loads more uniformly with a skewed base and by achieving better surface contact conditions with flat bearing lands. The Lewis Laboratory of NACA has found that skewing the base increases the operating life of cermet blades greatly in their full-scale engine tests. Pratt and Whitney Aircraft have recommended flat attachment surfaces as a result of their investigations in this field.

Comparative test results taken from Table 1 indicate that, for those specimens which failed in bearing, the skewed base withstood 28% greater load. However, very few of either type failed in bearing. Tension and bearing fractures in the base neck, and tension fracture in the blade root fillet are shown in Figures 8, 9, and 10. The majority of the dovetail specimens failed in tension across the base neck, which is the anticipated type and location of fracture, while the majority of the skewed dovetail

specimens failed in the blade root fillet at an average load of only 88% of the majority of the dovetail type and only 90% of the load sustained by those dovetail specimens that also failed in the blade root fillet. The explanation for these results is not readily apparent, and a thorough inspection is required of several of each type of specimen to determine the validity of a direct comparison of the test results.

Inspection of the skewed dovetail specimens reveals that the centroidal axis of the blade does not lie in the plane of the center-line between the bearing lands but is at an angle with it. This causes bending loads in the blade and blade root fillet under centrifugal load. The blade is canted so as to increase the tension load on the concave side of the blade root fillet which means that the leading and trailing edge tension loads are increased. The leading edge overhangs the root platform in the skewed base design, and the platform is quite thin and unsupported in this region. In addition, the root platform of the skewed dovetail specimen is 15% thinner than that of the dovetail specimen as shown by inspection. It appears reasonable to assume that, in combination, these factors could readily result in root fillet failure of the skewed dovetail specimens. It is presumed that the misalignment of the blade and bearing lands occurred while grinding the bearing lands due to not locating the specimens in the fixture properly. It is further presumed that if the skewed dovetail attachment were redesigned to incorporate a slightly thicker root platform and were fabricated to eliminate bending loads, it would demonstrate a similar superiority in overall strength with respect to the dovetail attachment as it currently does in regard to bearing strength.

Additional points of interest resulting from this simulated test program are the consistency of the data from successive tests of identical specimens in view of the use of inexpensive ceramic material and of a relatively simple test rig, and the close relationship of the attachment strength to the blade root strength of the dovetail design. One-quarter of these specimens failed in the blade root at an average load only 1% less than those that failed in the base neck.

Modification of Dovetail Design

The proportions of the dovetail base attachment are based upon data from Figure 1 for the maximum load factor.

Figure 1 resulted from tensile tests of rectangular plastic specimens in a universal testing machine. A polariscope was used to insure uniform loading in the entire notch and bearing land region. These ideal conditions result in the bearing limit curve showing maximum load factors which are difficult to realize in an attachment which is loaded non-uniformly by an airfoil-shaped blade.

An analysis of the dovetail base is made to determine what the load distribution on each bearing land is and what modifications can be made to improve it. The load distribution analysis is an approximate one since it is based upon the summation of the loads developed in radial columns without consideration of the proportion of load that is transferred to adjacent columns. This kind of approximation results in load distributions which are worse than would actually occur.

The root platform is divided into a grid of squares such that there are 20 squares in the chordwise direction and 11 squares perpendicular thereto. This grid is extended along the length of the blade such that the corners lie in radial lines. The squares thus become rectangles of more unequal proportions from blade root to tip. Large scale drawings are made of several cross-sections of the blade and oriented in true position on the grid for the radius at which the cross-section is located. These drawings are superimposed in adjacent pairs and the blade volume and centrifugal load within each column is calculated. This process is repeated for each pair of sections from tip to root and the individual load values are summed up to give the total load at the root for each column. The total of all the column loads is checked against the previously computed total blade load. The moment of each column load about the neutral axis of the attachment bearing lands is calculated and the bearing land reaction loads are obtained for each of the 20 rows of columns in the chordwise direction.

The results of this analysis indicate that rotating the base and bearing lands about the centroidal axis of the blade should improve the load distribution. Consequently, the bearing land load distributions are calculated for several angles of base rotation from zero to twenty degrees. The load distribution for fifteen degrees is considered to yield the best overall picture and is used for the skewed dovetail base configuration. The calculated load distributions for

no rotation and for 15 degrees rotation are shown in Figure 11. The peak load intensity on the convex side can be reduced by moving the blade on the base, but this is not recommended since it would introduce bending loads into the neck of the base.

The unit bearing stress on the lands is a function of the area in contact and also depends upon the absence of local surface conditions which cause concentrations. The former is determined by the proportions of the base and notch but the latter is determined primarily by the accuracy with which the contacting surfaces are fabricated. The blade base contour would undoubtedly be ground and the rotor segment slots would be broached in production. The accuracy and particularly the consistency during production runs with each of these fabricating techniques should be better for flat surfaces rather than curved. It is believed, therefore, that the incorporation of flat bearing lands in the design of the dovetail base in conjunction with rotating the base should make the realization of the maximum load factor shown in Figure 1 quite probable. Consequently, flat bearing lands subtending an angle of 60 degrees are incorporated in the design of the skewed dovetail base.

Tests conducted to establish the superiority of the skewed dovetail base with flat bearing lands over the plain dovetail base are not conclusive for the reasons given in the section of this report entitled "Dovetail vs. Skewed Dovetail Specimens".

Temperature Distribution

Radial temperature distributions for several gas temperatures and two rotor cooling conditions are computed for the rotor disk and blades of the small auxiliary gas turbine which is used as a reference throughout this study. These data are for use in making an analysis of the temperature-vs-service life to be expected from the dovetail base attachment. The calculations are based on a dovetail attachment with a blade neck width-to-rotor segment neck width (d_b/d_r) ratio of approximately unity. The method of calculating the temperature distributions are adapted from references 5,6, and 7. Heat transfer coefficients are obtained using the method of reference 8 and gas property and gas flow data supplied by the turbine manufacturer.

Temperature distribution curves for the turbine wheel without special cooling fins are shown in Figure 12 for effective gas temperatures of 1300, 1500, and 1800° F. Temperature distribution curves for the wheel with cooling fins on the rim are shown in Figure 13 for effective gas temperatures of 1300, 1500, 1800, and 2200° F. Effective gas temperatures are used since they are involved in the calculations. Inlet gas temperatures are approximately 5% or 65° to 110° F. higher than the effective gas temperatures shown. Rim cooling fins of adequate strength are calculated to increase the heat transfer coefficient from the disk to the cooling air by a factor of 4 or from $q_o = 30$ to $q_o = 120$. The cooling air temperature is assumed to be stabilized at 200° F. in all cases. The heat transfer coefficient from the hot gas to the turbine blade is computed to be constant at a value of $q_1 = 247$ BTU per hour per square foot per degree Fahrenheit. Other simplifying assumptions made to facilitate calculations are:

(1) Calculations are made on the basis of dividing the wheel into five sections i.e. blade, base above neck, base below neck, rotor segment, and rotor disk.

(2) Constant mean values of the heat flow area, perimeter, thermal conductivity, and heat transfer coefficients are used for each section.

(3) No temperature gradients other than radial are considered.

(4) Radiation effects are neglected.

(5) Cooling on both sides of the turbine rim and disk is assumed.

(6) The blade tip is insulated and the gas temperature is constant along the blade span.

In order to determine more accurately the temperatures in the critical region of the attachment, a two-dimensional distribution is calculated using the relaxation method of reference 9. A typical distribution is shown by the isothermal lines of Figure 14 for an effective gas temperature of 1600° F. without rim cooling. The temperatures used in the detail analysis of the dovetail base attachment are obtained in this manner.

Cermet Material Data

Titanium carbide in conjunction with metallic binders is the most advanced cermet material for which data adequate for design purposes is available. This basic material has been combined with many different combinations of binders by two principal techniques, i.e., pressing and sintering as dry mixed powders or infiltrating the TiC matrix with molten metal during final sintering. Both methods have produced very satisfactory materials from the high temperature strength standpoint. In general, the high nickel content materials show the best overall combination of properties. They combine high temperature strength with satisfactory oxidation resistance and thermal shock resistance. However, they significantly lack impact strength which is a universal shortcoming of all the brittle cermet materials for which data are available.

Of the several remaining types of cermet materials, the borides appear to show the greatest promise. Zirconium boride compositions show very good high temperature strength and thermal shock resistance but they start to decompose in an oxidizing atmosphere after 250 hours. Sufficient data are not available to evaluate the chromium boride compositions. However, preliminary information indicates that high temperature strength equal to other cermets is possible with satisfactory oxidation and thermal shock resistance and, most hopeful of all, considerably more ductility. More ductility indicates the possibility of greater resistance to impact, the lack of which is the one major reason why the present cermet materials probably will not find wide use in gas turbine blade applications.

The compositions of several representative cermet materials are given in Table 2 to the extent that they are available. Physical property data as obtained from the manufacturers are furnished in Table 3 for several materials. Stress-rupture curves representing the best available data for the most promising materials are given in Figure 15. It is readily apparent that the availability of data is limited and that such information as is available is sketchy and incomplete. It is also noted that comparison of material properties is difficult because of the many different methods of testing for a given characteristic which are employed by the manufacturers of these materials. Standardization of test procedures would facilitate comparison and selection of these materials.

Detail Analysis of Dovetail Attachment

The dovetail attachment is subjected to a more detailed analysis to determine its maximum theoretical temperature vs. service life performance under the design load conditions for the small auxiliary gas turbine. This analysis is carried out for each of the three most promising cermet materials for which data were available and also for each of the two turbine cooling conditions.

Most turbine blade stress-rupture failures occur in one of three places; in the blade itself, in the blade base neck, or in the rotor segment neck. In this analysis it is assumed that the blade dimensions and proportions are established by turbine performance requirements and are held constant during the study. To determine the location and time of failure of the blade at any given gas temperature, it is necessary to make a plot relating the operating stress in the blade and the allowable stress for the material at the local temperature corresponding to the effective gas temperature. Such a plot is shown in Figure 16 for K 162-B material at an effective gas temperature of 1800° F. with rim-cooling (q_o = 120). The operating stress curve is calculated at a speed of 36,000 RPM and using the density of the material under consideration. The allowable stress curves for 10,100, and 1000 hours are taken from stress rupture data for the cermet material at the local temperature obtained from the temperature distribution curves. For the conditions shown in Figure 16, the blade will fail at a radius of approximately 0.252 feet after about 750 hours of operation at 1800° F. Cross-plots are made to determine the time and location of failure with greater accuracy and the resulting data are plotted as the time-vs-temperature curve for blade failure of Figure 18 for q_o = 120. This procedure is repeated for each material and for both rotor cooling conditions and result in the six blade failure curves of Figures 18, 19, and 20.

The maximum strength of the attachment will occur when it is proportioned such that the blade base neck and the rotor segment neck are equal strength. The optimum ratio between the blade base neck and the rotor segment neck varies with the operating temperature, time-to-failure, and the cermet material used because of the difference in temperature gradients and the variation in slope of the stress - rupture curves for the different materials. The optimum ratio is determined for each set of conditions (material and cooling) as shown in Figure 17 for K162-B material and rim cooling. It indicates that for a 10 hour life an attachment with a

D_b/d_r ratio of 1.76 will have equal strength in the blade base and rotor rim and will withstand a maximum effective gas temperature of 2200° F. At greater D_b/d_r ratios the rotor rim will fail and at lesser ratios the blade base will fail. The same data are furnished for 100 hour and 500 hour life and the optimum points are used to plot the temperature-vs-life curves for attachment failure (in this case with cooling fins) shown on Figure 18. Similar plots are prepared for each ofthe materials and for both cooling conditions and result in the attachment failure curves of Figures 18, 19, and 20 for optimum D_b/d_r ratio. Additional curves are plotted for D_b/d_r ratios near the optimum to indicate the sensitivity of attachment strength to small changes in D_b/d_r ratio.

The curves illustrated by Figure 17 are prepared using the following relationships.

For equal strength:

$$\left(\frac{D_b}{d_r}\right)_{Opt.} = \frac{1}{(d_b/D_bK_f)} \left(\frac{S_r}{S_b}\right) \left(\frac{P_b}{P_r}\right) \qquad (3)$$

For rim failure:

$$\left(\frac{D_b}{d_r}\right)_{Max.} = t\left\{\frac{2\pi R_r}{55}\right\}\left\{\frac{S_r}{P_r}\right\} - 1 \qquad (4)$$

For blade base failure:

$$\left(\frac{D_b}{d_r}\right)_{Min.} = \frac{1}{t\left\{\frac{2\pi R_r}{55}\right\}\left\{\frac{d_b}{D_bK_f}\right\}\left\{\frac{S_b}{P_b}\right\} - 1} \qquad (5)$$

Where:

D_b = blade base width at bottom of notch
d_b = blade base neck width
d_r = rotor segment neckwidth
t = thickness of blade base and rotor rim
R_r = radius from rotor axis to rotor segment neck
$\frac{d_b}{D_bK_f}$ = blade base load factor (.462 for optimum dovetail)
S_b = stress-rupture strength of cermet material in blade neck
S_r = stress-rupture strength of Timken 16-25-6 material in rotor segment neck.
P_b = design operating load in blade base neck
P_r = design operating load in rotor segment neck

These relationships are derived from the stress equations at each critical point and the geometric relationship that $D_b + d_r = 2\pi R_r/55$ where 55 blades are used in the turbine wheel. Data from the temperature distribution calculations in conjunction with stress-rupture data from the three cermet materials and for the disk alloy, Timken 16-25-6, are used to obtain solutions to Equations (3), (4), and (5). The solutions are plotted on curves similar to Figure 17, and the optimum solutions are in turn plotted to form the temperature-vs-life curves of Figures 18, 19, and 20.

Figure 18 shows the theoretical maximum temperature-vs-life performance of the dovetail attachment and K162-B material when used in a small auxiliary gas turbine. The maximum effective gas temperature for 100 hour service life is limited by the attachment without cooling to 1820° F. With rim cooling it is limited by the blade itself to 1860° F. A small amount of rim cooling will apparently increase the attachment temperature limits to provide some margin over the blade limit.

Figure 19 shows the temperature-vs-life performance of K161-B material under identical circumstances. The maximum temperature for 100 hours is limited by the attachment without cooling to 1820° F. With cooling fins it is limited by the blade to 1920° F. It is apparent that rim cooling fins permit a substantial increase in temperature with this material.

Figure 20 shows the temperature-vs-life performance of TC-66-1 material under the same conditions. The maximum temperature for 100 hours without cooling is limited by the attachment to 1820° F. With cooling fins it is limited by the blade to 1915° F.

It is readily apparent that there is little difference as regards strength between the cermet materials included in this analysis. This conclusion is emphasized when the limited nature of the stress-rupture data is considered. Several extrapolations of basic data were required to complete the analysis and since the accuracy of extrapolated physical property data is questionable, this factor alone might well change the comparison of these materials. However, it is also apparent that the dovetail attachment when applied to a small gas turbine using brittle blade material will permit the use of higher gas temperatures without cooling. With rim cooling it appears probable that the attachment

strength can be made to exceed the blade strength with an additional increase in operating temperature. These increases are more pronounced for long service-life operation due to the relatively flat stress-rupture characteristics of the cermet materials.

Additional Considerations

In addition to the basic attachment problem associated with the application of brittle materials as gas turbine blades, there are several other problems or effects to be considered. The rotor disk is subjected to smaller centrifugal loads due to the low density of the cermet but receives more heat from the blades due to increased thermal conductivity. As the rotor rim expands and contracts with temperature changes the blade bases do not change at the same rate due to different coefficients of thermal expansion. The blades must be installed with sufficient clearance to insure that they do not fail as a result of overconstraint. Alloy blades are commonly retained in the rotor rim by ball-peening the ends of the blade bases or the rotor segments. This cannot be done with brittle material blades because they will not peen and they are extremely sensitive to the stress concentrations resulting from peening the rotor segments.

A rotor disk profile is designed for the small auxiliary gas turbine with cermet blades and subjected to stress analysis with design loading at 1600° F. without rim cooling, and at 1800° F. and 2200° F. with cooling fins. The methods used are taken from reference 10. The profile and the stress conditions are shown in Figure 21. The disk is thinner and lighter than its counterpart using alloy blades at an effective gas temperature of approximately 1400° F. It is noted that plastic flow of the rotor rim material occurs only with the 2200° F. temperature.

A brief analysis of the thermal expansion problem indicates that the blade bases will tighten in their slots due to differential expansion, however, a minimum clearance of .002 inch is sufficient to prevent overconstraint in the case of the small auxiliary gas turbine. The use of a ductile insert of approximately .005 inch thickness on each side of the blade base should help to eliminate overconstraint and crushing. The progressive crushing effect resulting from plastic flow of the rotor rim after cycling the engine does not appear to be a serious problem in this case due to the absence of plastic flow at practical operating temperatures.

A satisfactory method of retaining the brittle material blades must be simple but must not cause any additional stresses in the blade base. Three suggested methods of retaining the blades are shown in Figure 22. The rivet type is simple and inexpensive but care is required to prevent cracking the bases while driving the rivets. The self-locking pin type is simpler yet, and while it increases the bearing land loads this should have a negligible effect. The snap-ring type is suggested to provide a quick method of removing and installing a complete set of blades. This may have advantages because of the fact that all blades may be destroyed if one blade fails due to the lack of impact resistance of the brittle material. Many other methods of retaining the blades could be suggested but these are representative of the possibilities and appear to be satisfactory for most applications.

CONCLUSIONS AND RECOMMENDATIONS

1. Brittle material blades can be satisfactorily attached to ductile rotor disks. The problems of stress concentration, distribution of attachment loads, differential thermal expansion, and retension can be solved by careful design of the attachment configuration, incorporation of a ductile insert, attention to fits and tolerances, and selection of proper retaining methods.

2. Substantial temperature increases are possible in turbines with cermet blades due to their excellent high temperature strength and their low density. Some cooling of the turbine is required to realize the full potential, but the simplest means of cooling, i.e., fins on the rotor rim, is adequate. Under such conditions cermet blades can be operated for 100 hours or more at inlet gas temperatures approximately 2000° F.

3. A dovetail type attachment is superior in strength to others considered because of its low stress concentration factor due to large notch radius. It is simple to fabricate and assemble. A modification of the dovetail attachment which includes rotating the base 15 degrees toward the convex side of the blade and which incorporates flat bearing lands is theoretically superior to the plain dovetail. The tests conducted to establish the relative merits of these modifications were inconclusive. However, it is recommended that the skewed dovetail attachment with flat bearing lands be given serious consideration as a superior design.

4. Nickel-plated, perforated copper screen is a thoroughly satisfactory ductile insert for use between the blade base and rotor segment. Woven brass screen and thin, copper sheet show good load distribution characteristics in tests but are not as consistently superior as are the perforated screen inserts.

5. Considerable savings of critical materials can be achieved by using cermet blades, since the cermets are low in strategic material content, and the highly alloyed rotor disks can be smaller and lighter.

6. Currently available data on cermets indicate that their impact resistance is very poor. Until further metallurgical research results in sizeable improvements in this property, it is unlikely that these materials will find wide use in gas turbine blade applications. Such research is recommended in view of the tremendous potential of these materials.

7. It is recommended that further tests be conducted to determine the validity of the analyses contained in this report with respect to maximum operating temperatures and operating service life. However, since full scale engine tests are required, it is recommended that such tests only be undertaken if lack of impact resistance is judged to be unimportant in the application under consideration, or if a cermet material having adequate impact resistance is available.

REFERENCES

1. Peterson, R. E.

Design Factors for Stress Concentration, Machine Design, March 1951.

2. Neuber, H. - "Kerbspannungslehre", Springer Verlag, Berlin 1937. English translation published by Edwards Co., Ann Arbor, Mich. 1946.

3. Meyer, A. J. Jr., et al - NACA Research Memorandum

4. Miklowitz, Jr. Elastic Waves created during Tensile Fracture, ASME Paper No. 52-A-10, 1952.

5. Wolfenstein, L. et al - Cooling of Gas Turbines, II, Effectiveness of Rim Cooling of Blades, NACA RM E7B11b March, 1947.

6. Brown, W. B. & Livingood, J.N.B. Cooling of Gas Turbines, VIII, Theoretical Temperature Distributions through Gas Turbine with Special Blades and Cooling Fins on Rim, NACA RM E7122a Feb. 1948.

7. Brown & Livingood Analysis of Spanwise Temperature Distribution in Three Types of Air-Cooled Turbine Blade NACA Report 994, 1950.

8. Hubbartt, J. E. Comparison of Outside-Surface Heat-Transfer Coefficients for Cascades of Turbine Blades, NACA RM E50C28, July, 1950.

9. Emmons, H. W. The Numerical Solution of Partial Differential Equations, Quarterly, Applied Mathmatics, October, 1944.

10. Manson, S. S. Direct Method of Design and Stress Analysis of Rotating Disks with Temperature Gradient, NACA Report No. 952, 1950.

TABLE 1 - TEST DATA

RUN NO.	SPEC.(1) NO.	DUCTILE INSERT	SOAK RPM.	FAILURE RPM.	FRACTURE		REMARKS (CRS holder unless noted
					TYPE	LOCATION	
1	C3	NONE	2500	11,500	Bear.	Neck	24ST holder
2	C7	NONE	5000	11,100	Bear.	Neck	24ST holder
3	C4	None	5000	11,600	Bear.	Neck	24ST holder
4	C11	None	5000	9,600	Bear.	Neck	CRS holder
5	C10	None	5000	9,200	Bear.	Neck	CRS holder
6&7	C5	None	5000	12,700	Bear.	Neck	24ST holder & retainer on root platform
8	C17	005 Cu Sheet	6000	11,000	Bear.	Neck	CRS holder
9	C18	005 Cu Sheet	6000	8,800	Bear.	Neck	X-Ray reject *
10	C19	None	6000	8,250	Bear.	Neck	
11	C20	010 Cu Sheet	6000	9,300	Tens.	Root fil.	Fracture not explained *
12	C21	010 Cu Sheet	6000	8,250	Bear.	Neck	X-Ray reject *
13	C22	010 Cu Sheet	6000	10,200	Bear.	Neck	
14	S2	010 Cu Sheet	6000	10,000	Bear.	Neck	1st airfoil blade
15	S3	010 Cu Sheet	6000	8,250	Bear.	Neck	X-Ray reject*
16	S4	010 Wov.Screen	6000	11,200	Bear.	Neck	
17	S5	010 Cu Sheet	6000	10,200	Bear.	Neck	Large chip off blade tip
18	S6	005 Cu Plating	6000	9,750	Bear.	Neck	Plating not well bonded *
19	C28	010 Wov.Screen	6000	11,500	Bear.	Neck	
20	C29	010 Wov.Screen	6000	9,700	Undet.	Above Neck	Base chipped-unusual fracture*
21	C23	010 Wov.Screen	6000	10,950	Bear.	Neck	
22	S10	010 Wov.Screen	6000	11,000	Bear.	Neck	
23	S9	010 Wov.Screen	6000	10,600	Bear.	Neck	
24	S11	010 Wov.Screen	6000	10,600	Bear.	Neck	Small chip at blade tip
25	S13	005 Cu Sheet	6000	9,450	Bear.	Neck	Chipped blade tip
26	S12	005 Cu Sheet	6000	8,200	Bear.	Neck	Low strength not explained *
27	S7	005 Perf.Screen	6000	11,000	Bear.	Neck	Chip at base of notch
28	S8	005 Perf.Screen	6000	9,600	Bear.	Neck	Gas hole in neck *
29	D4	005 Perf.Screen	6000	15,200	Tens	Neck	1st Dovetail-stopped twice for inspection
30	D2	005 Perf.Screen	6000	15,500	Tens	Neck	Small gas hole in neck

REVISED:

TABLE 1 (Cont) - Test Data

RUN NO.	SPEC(1) NO.	DUCTILE INSERT	SOAK RPM.	FAILURE RPM.	FRACTURE TYPE	FRACTURE LOCATION	REMARKS (CRS holder unless noted
31	D14	005 Perf.Screen	6000	15,500	Tens	Root Fil.	Small holes in neck
32	D3	005 Perf.Screen	7500	12,300	Bear.	Neck	Blade tip not ground off
33	D15	005 Perf.Screen	7500	9,200	Undet.	Blade	Failed at 2/3 blade span *
34	D7	005 Perf.Screen	6000	14,700	Tens.	Neck	Fract.slightly spalled
35	D12	005 Perf.Screen	6000	15,400	Tens.	Root.Fil	Blade tip not ground off
36	D10	005 Perf.Screen	6000	14,300	Tens.	Neck	
37	D8	005 Perg.Screen	6000	17,100	Tens.	Neck	Strongest specimen
38	D1	005 Cu Sheet	6000	Stopped for severe vibration-test rig repaired			
38A	D1	005 Cu Sheet	6000	16,400	Tens.	Neck	Tract. spalled
39	SD9	005 Perf.Screen	6000	14,400	Tens.	Root Fil	1st Skewed Dovetail
40	SD5	" " "	6000	13,500	Bear	Neck	Fracture spalled
41	SD4	" " "	"	14,200	Tens.	Root Fil,	)Platform too thin-
42	SD8	" " "	"	14,400	"	"	)Blade axis not
43	SD10	" " "	"	15,300	"	"	) radial through
44	SD18	" " "	"	14,500	"	"	) base center
45	SD6	" " "	"	14,300	Bear	Neck	Fracture spalled

* These runs are not representative and arenot included in the analysis of these data.

(1)Specimen numbers include the type of specimen i.e. C for Calibration
S for Standard
D for Dovetail
SD for Skewed Dovetail

REVISED.

TABLE 2

COMPOSITION OF CERMET MATERIALS

SOURCE OF DATA	MATERIAL	% COMPOSITION BY WEIGHT							
		TiC	CbTaTiC	Ni	Mo	Al	Cr	Co	Fe
Thompson Products	TC-864-I	30%		38.5%*			7.5%*		3.5%*
Kennametal	K 158-B	64%	6%	30 %					
	K 161-B	62%	8%	30%					
	K 162-B	64%	6%	25%	5%				
	K 163-B	57%	8%	30%	5%				
	K 153-B	54%	6%	40%					
Amer. Electro Metal Corp.	Ecrolite I	Primarily Zirconium Boride							
	Ecrolite III	Primarily Chromium Boride							
Pratt & Whitney	JR	42%	8%	33.8%	12.7%	3.5%			
	JR-5	54%	3%	27 %	10.2%	2.8%			
	JR-6	46%		46 %	2 %	2 %		4%	

* Constituents of Inconel

TABLE 3

PHYSICAL PROPERTIES OF CERMET MATERIALS

	TC-[illegible]-I	K 152-B	K 162-B	Porcelite
Source of Data	Thompson	Kennametal	Kennametal	Porcelite
Modulus of Elasticity (PSI)		47x10^6	39x10^6	31x10^6
Thermal Expansion (in/in/^{o}Fx10^{-6} to 1200 ^{o}F)		5.3x10^{-6}	5.3x10^{-6}	5.7x10^{-6} (1000 ^{o}F)
Thermal Conductivity (btu/hr)(sq.ft)(^{o}F per ft.)		18.6	17.5	10.0
* Oxidation Resistance (wt. Change after 100 hrs (mg/cm^2)	7 (2,000^{o}F)	11 (1,800^{o}F)	7 (1,800^{o}F)	3 (2,000^{o}F)
* Thermal Shock	Good	Good	Good	Good
Charpy Impact Strength 3/16" at 1000^{o}F (in. lb.)	6.3,4.9 (Cone are alloys)	1.6,3.8 considered	3.2,2.2 good, compared to	
Density (lb./in^3)	.217	.207	.220	.10
Stress Rupture				
1800 ^{o}F 10 hr. (PSI)	31500	26000	41000	
100 hr	38000	19000	31500	
500 hr	30500		24000	
1500 ^{o}F 10 hr (PSI)	22500	13000	23500	25,000
100 hr	15000	9500	13000	18,500
500 hr	11500		9500	
1000 hr				14,000

* Test conditions vary over a wide range. Numerical results can be misleading.

REVISED:

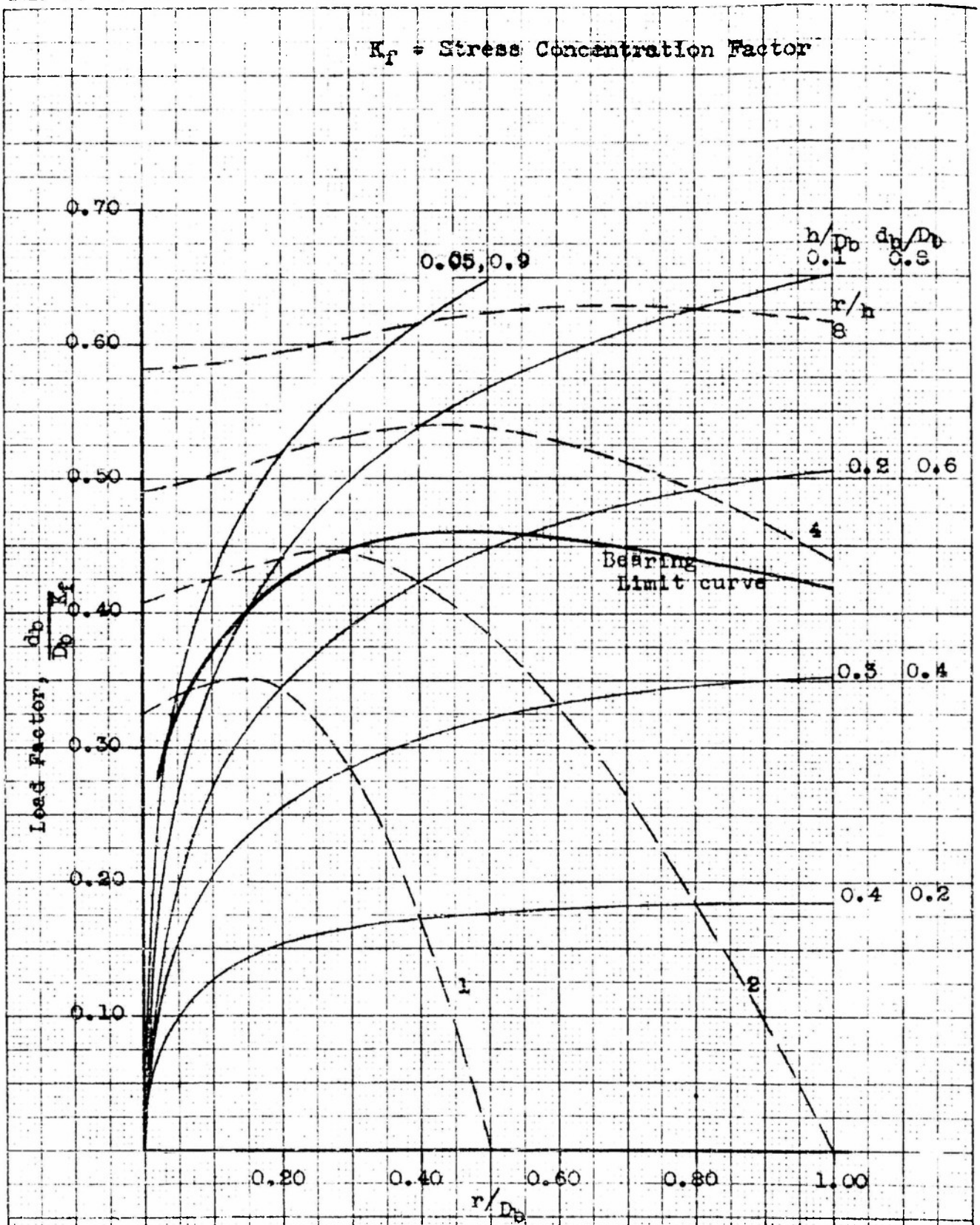

Figure 1. - Theoretical Design Chart relating stress concentration load factor with notch parameters and showing bearing stress limitation.

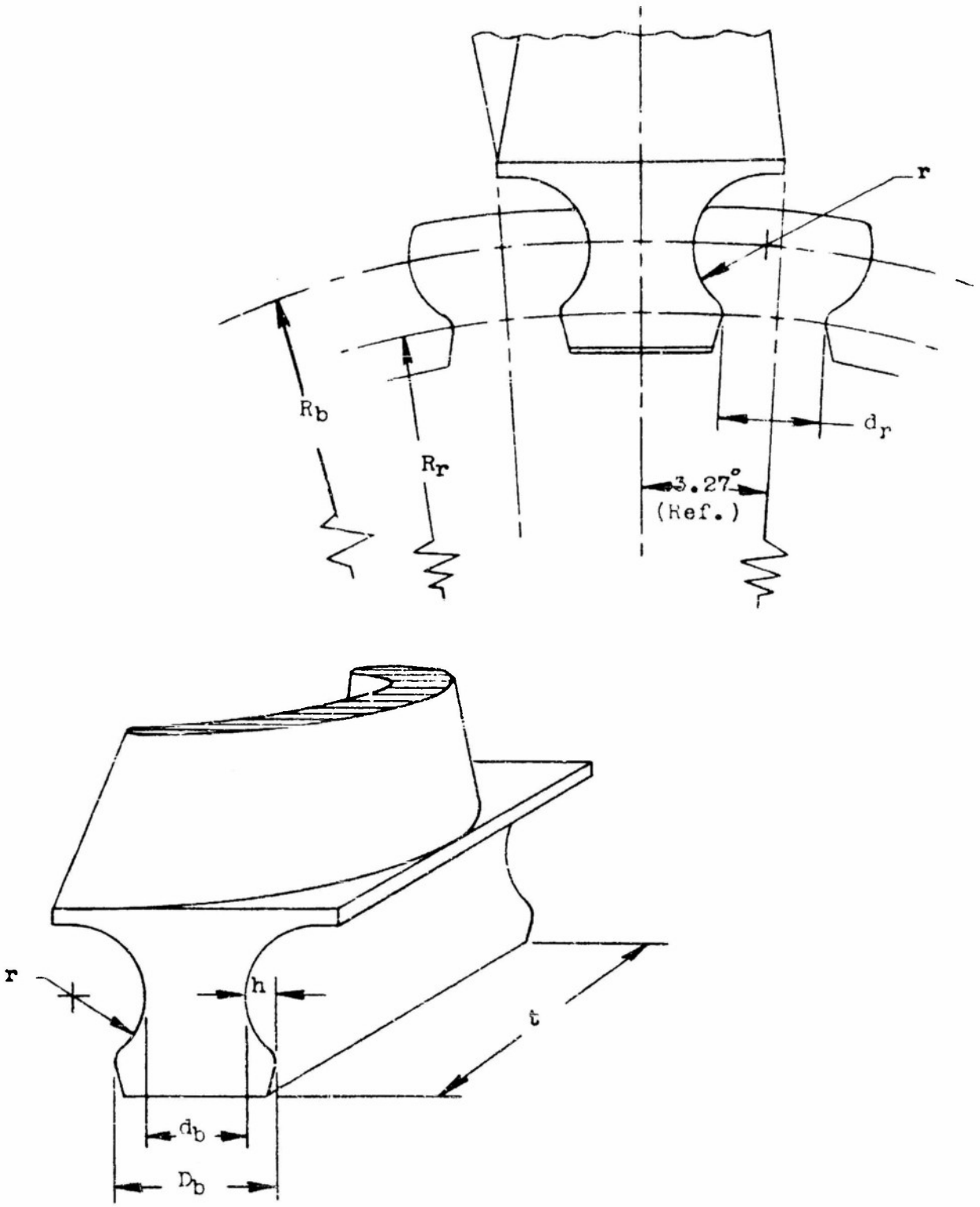

Figure 2.- Notation of blade base and rotor rim segment dimensions.

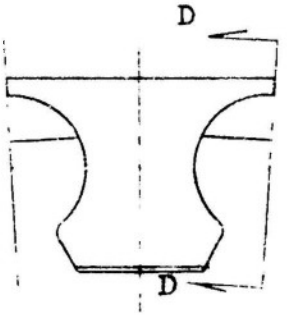

Dovetail

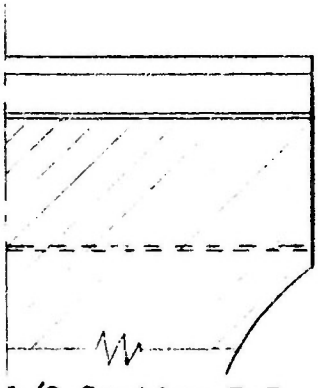

1/2 Section D-D

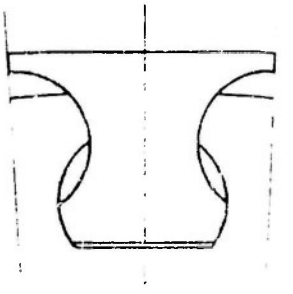

Pin-in-Compression or Interlock

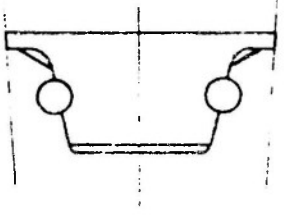

Pin-in-Longitudinal Shear

FIGURE 3 - Attachment types investigated in preliminary analysis (approximately to same scale)

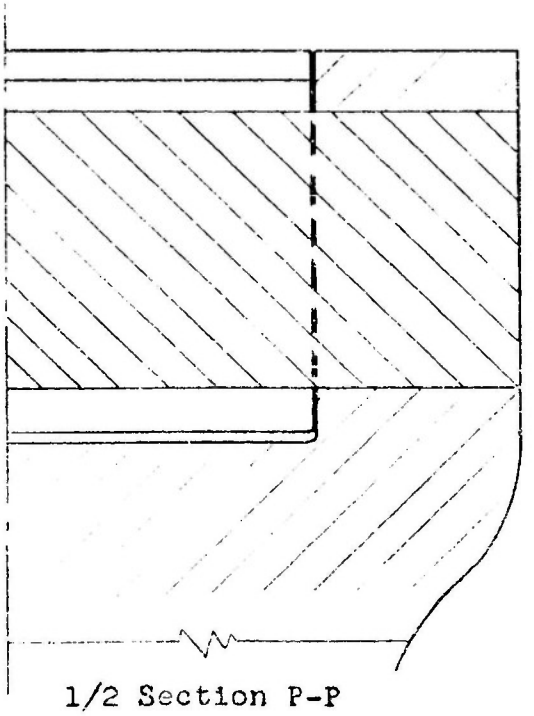

1/2 Section P-P

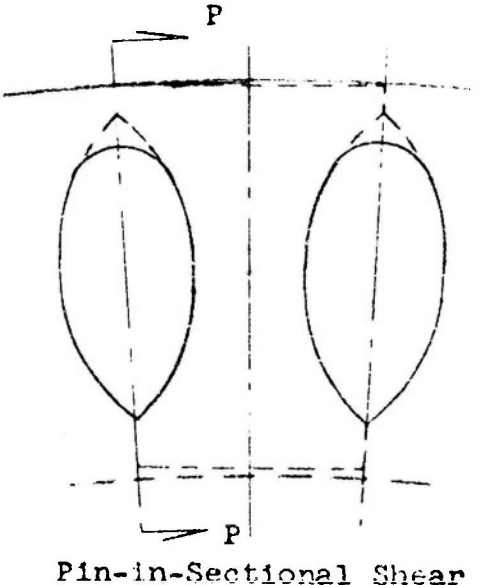

Pin-in-Sectional Shear

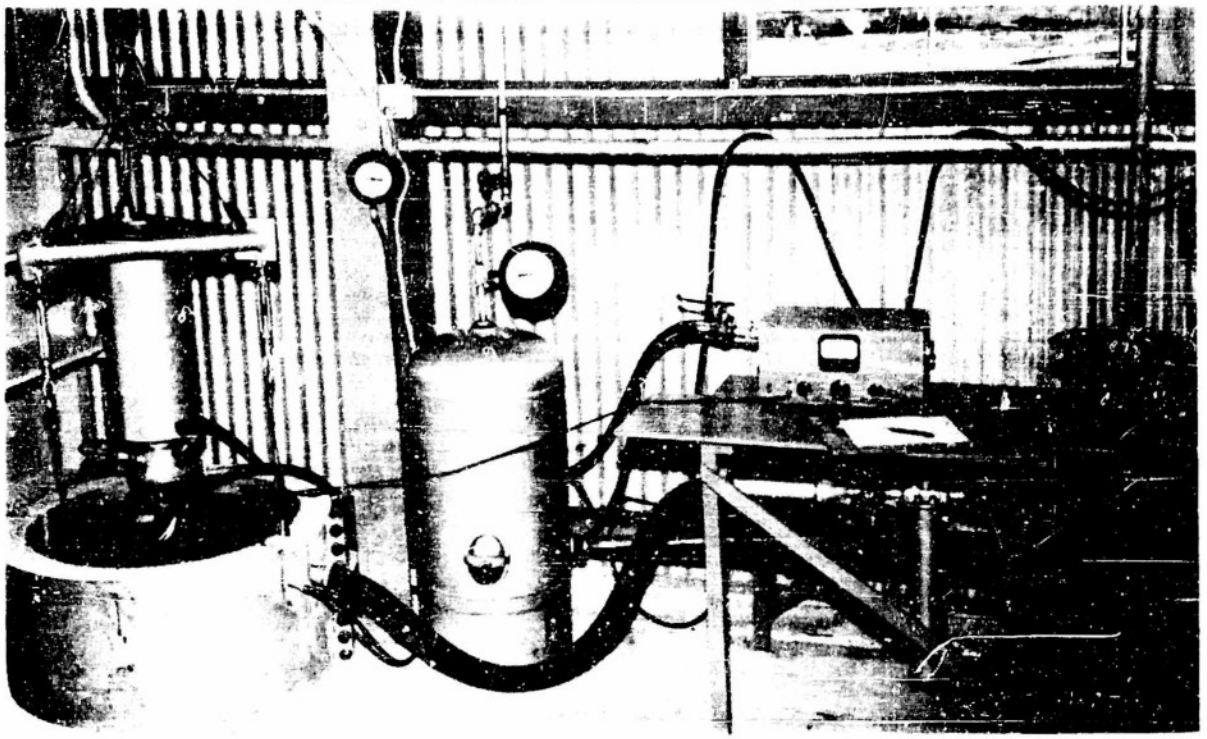

Figure 4(a) - Test Installation, showing l. to r.: protective barricade, test chamber, hoist equipment, vacuum gage, air tank and gage, control valves, techometer, vacuum valves, filter, and pump.

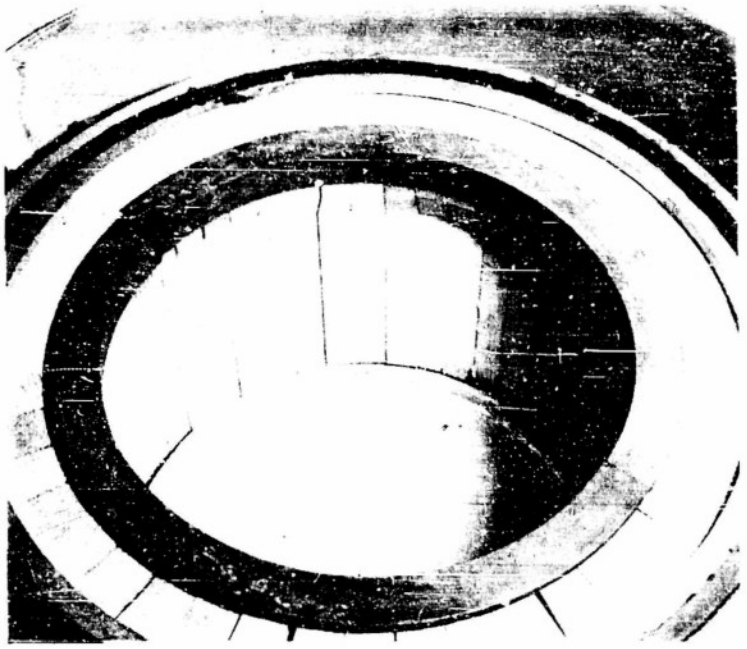

Figure 4(b) - Test Chamber Interior, showing: vacuum seal, wooden safety blocks, block retaining rings, and portion of barricade.

Figure 4(d) - Test Chamber Top showing: inspection windows, drive assembly, air brake, muffler, tachometer head and power supply.

Figure 4(c) - Test Wheel Assembly, showing l. to r.: counterweight, wheel, specimen and holder, and method of assembly.

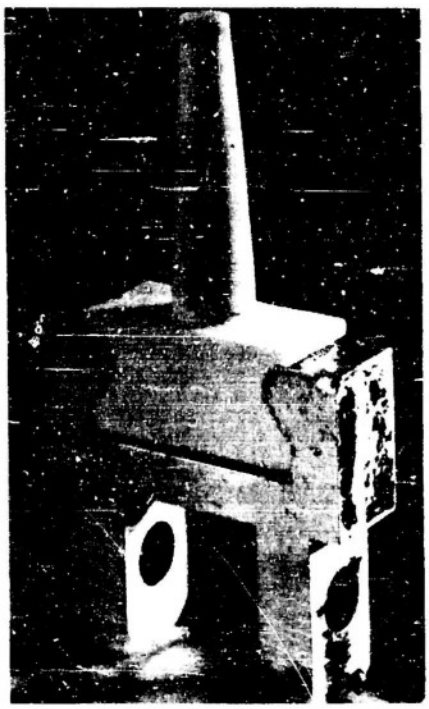

Calibration

Standard

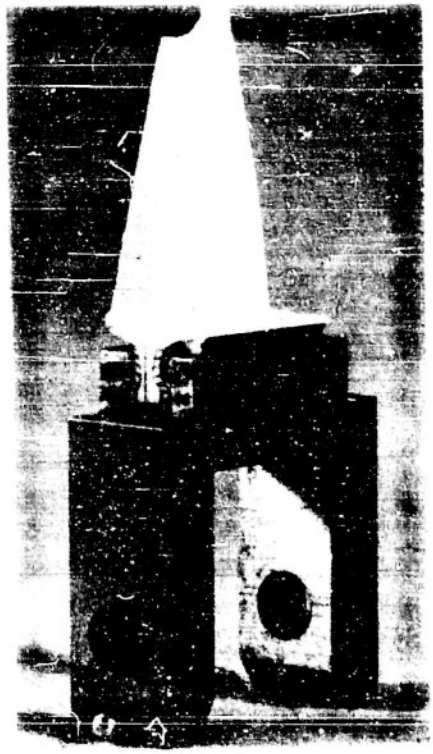

Dovetail with perf.screen insert (rejected spec.)

Skewed Dovetail (perf. screen insert)

Figure 5 - Test specimens and holders

Figure 6 - Specimen after test showing reassembled major fragments and location of fractures.

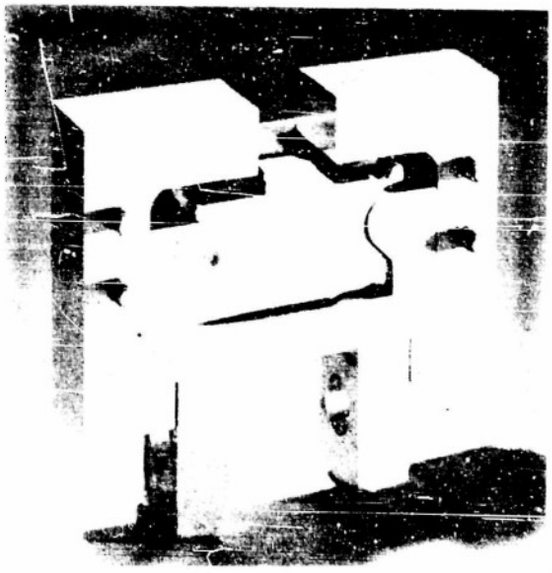

Figure 7 - Specimen base retained after Run 7 showing initial failure in bearing just below neck of base (on left).

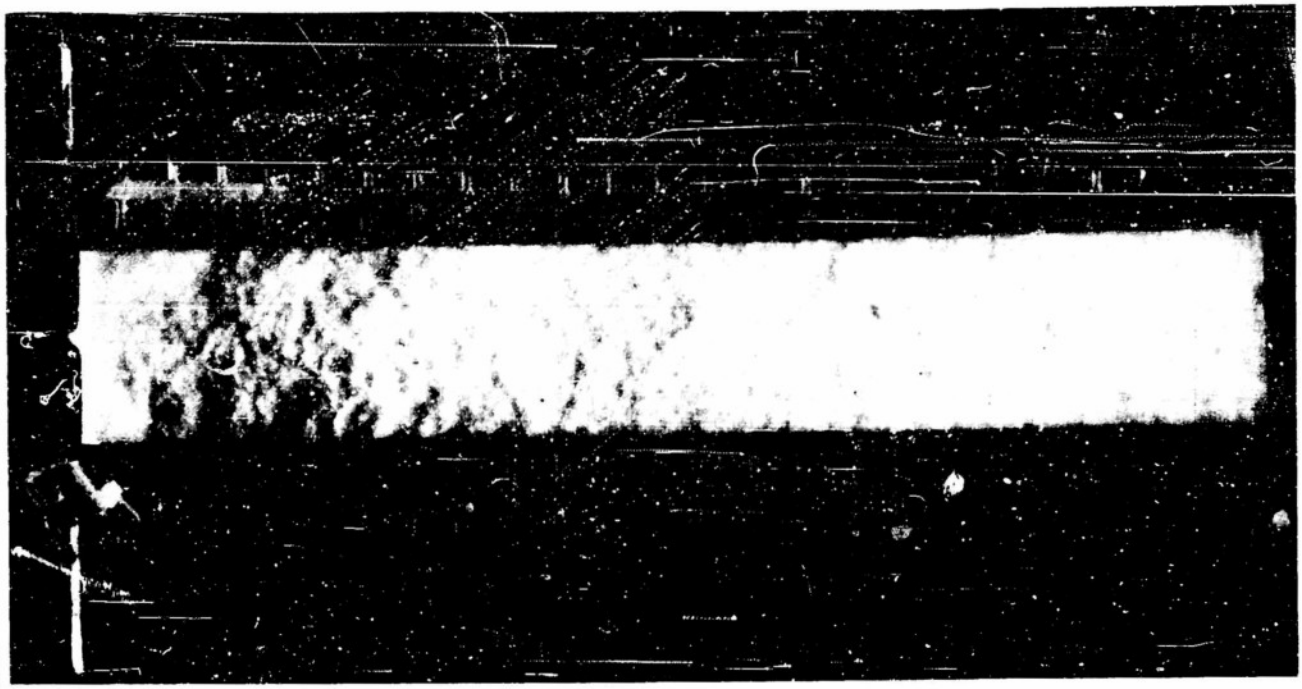

Plan View

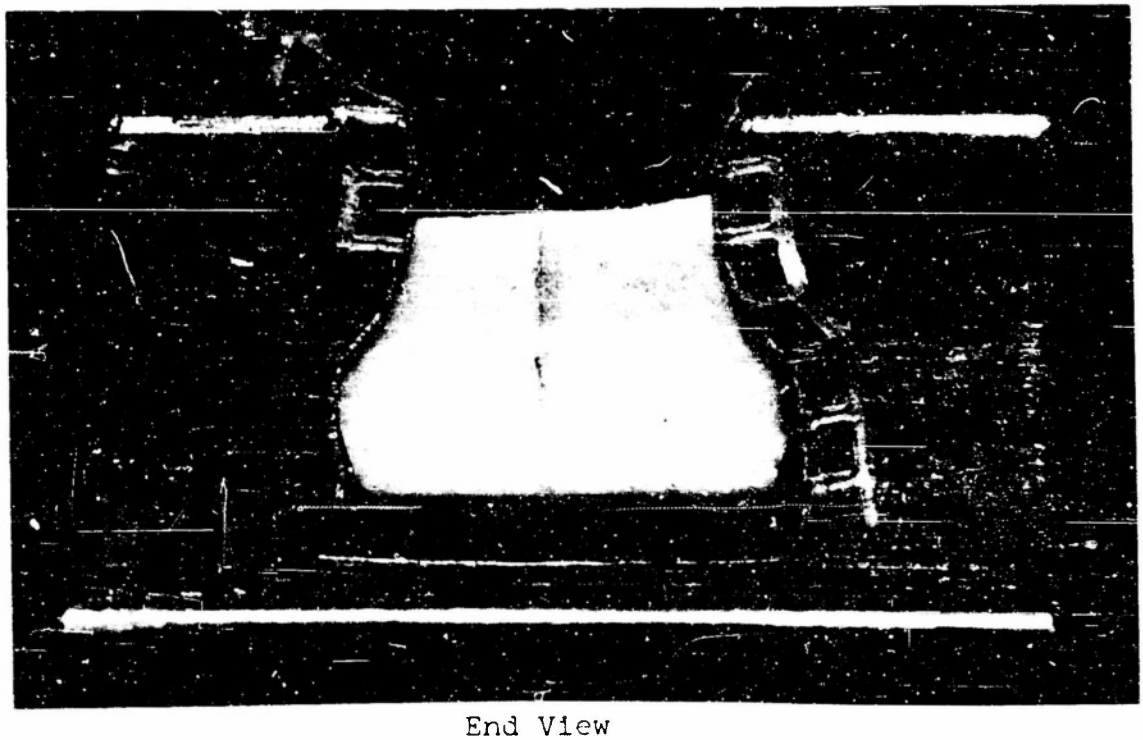

End View

Figure 8 - Typical tension fracture in neck of base, dovetail specimen (approx 9 x size)

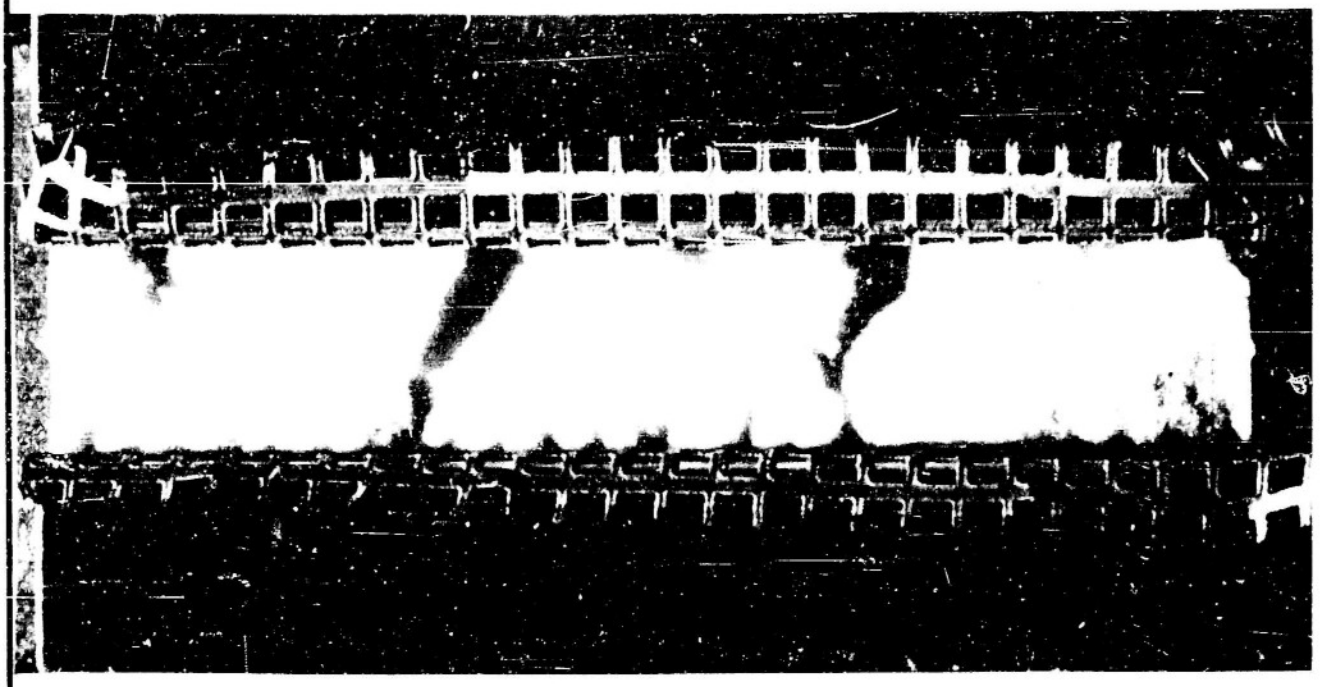

Plan View

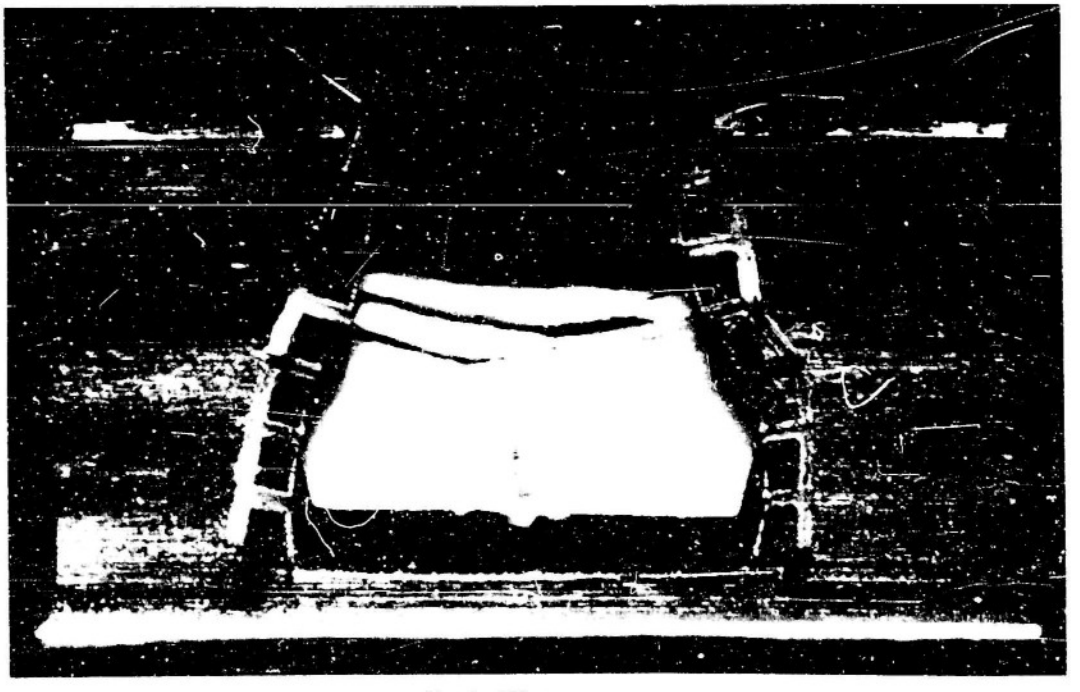

End View

Figure 9 - Typical bearing fracture in neck of base, dovetail specimen (approx. 9 x size).

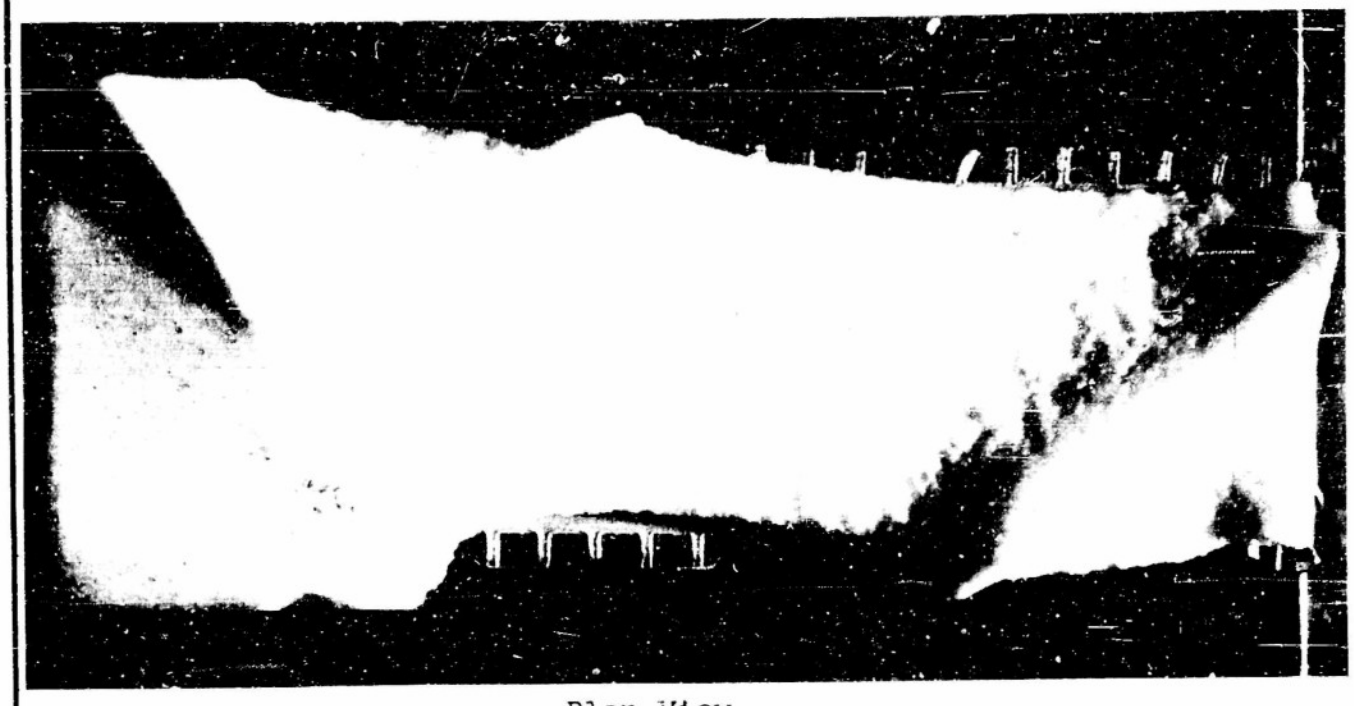

Plan View

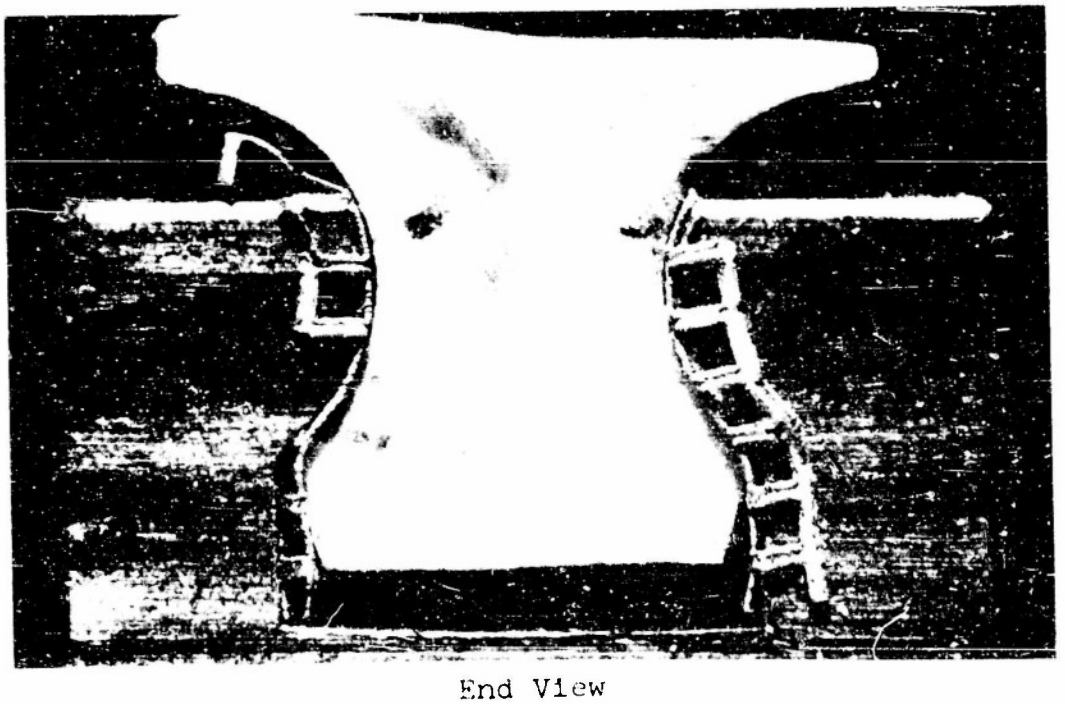

End View

Figure 10 - Typical tension fracture in blade root fillet - dovetail specimen (approx. [illegible] x size).

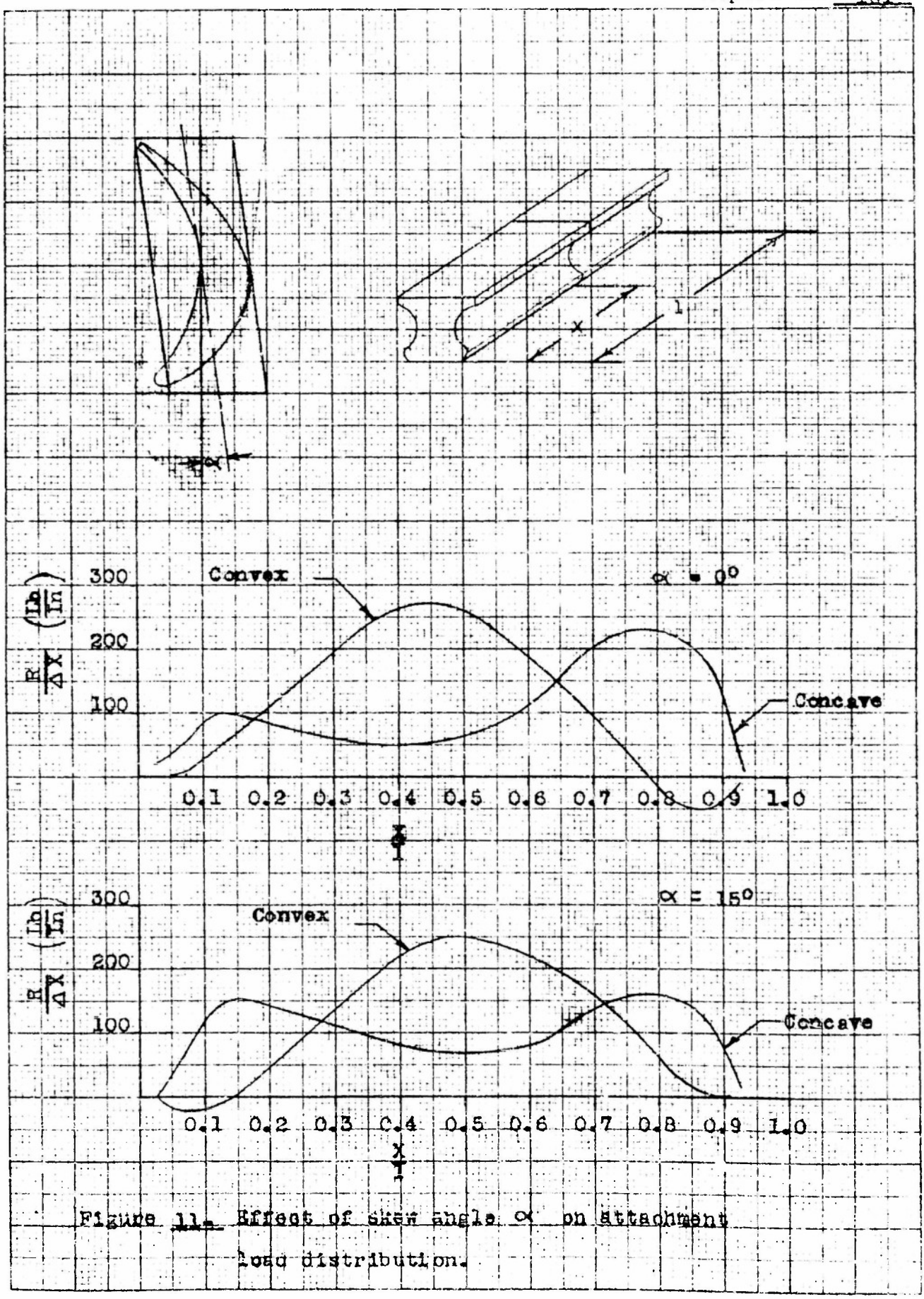

Figure 11. Effect of skew angle α on attachment load distribution.

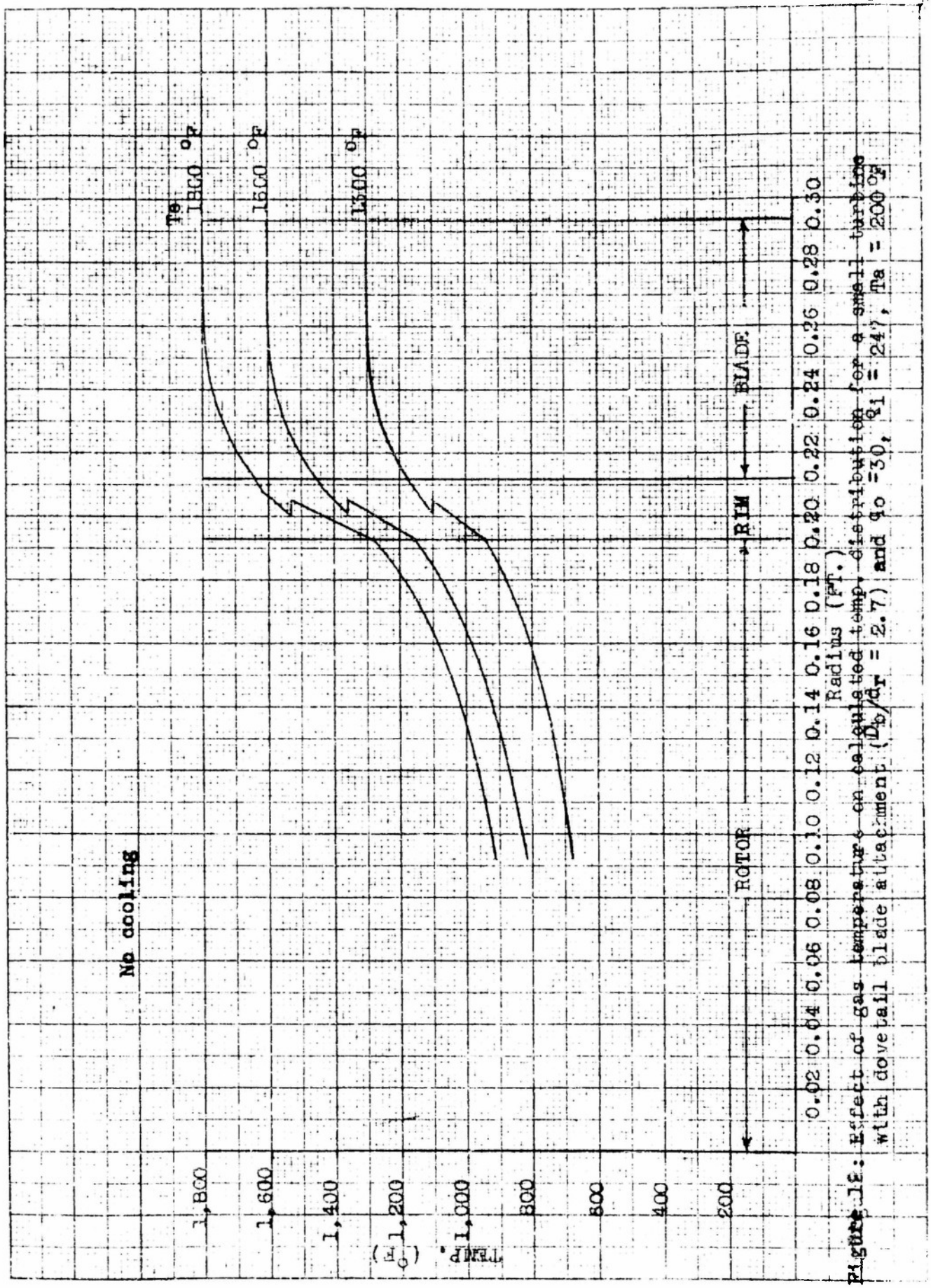

Figure 15: Effect of gas temperature on calculated temp. distribution for a small turbine with dovetail blade attachment ($D_o/d_r = 2.7$) and $\varphi_o = 30°$, $\varphi_i = 24°$, Ta = 200 °F

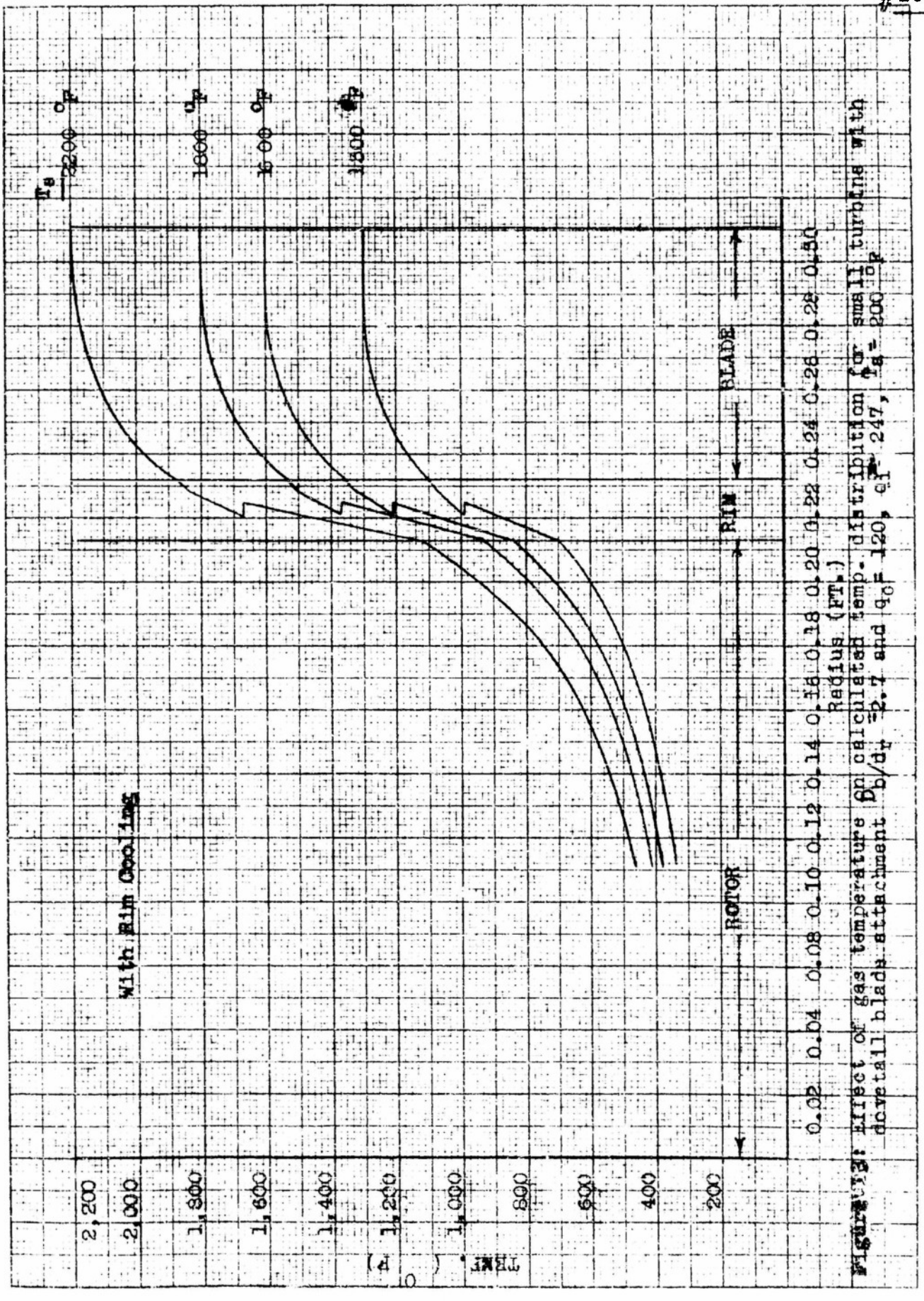

Figure 23: Effect of gas temperature on calculated temp. distribution for small turbine with dovetail blade attachment D_b/d_r = 2.7 and q_o = 120, at T_s = 247, T_s = 200 °F

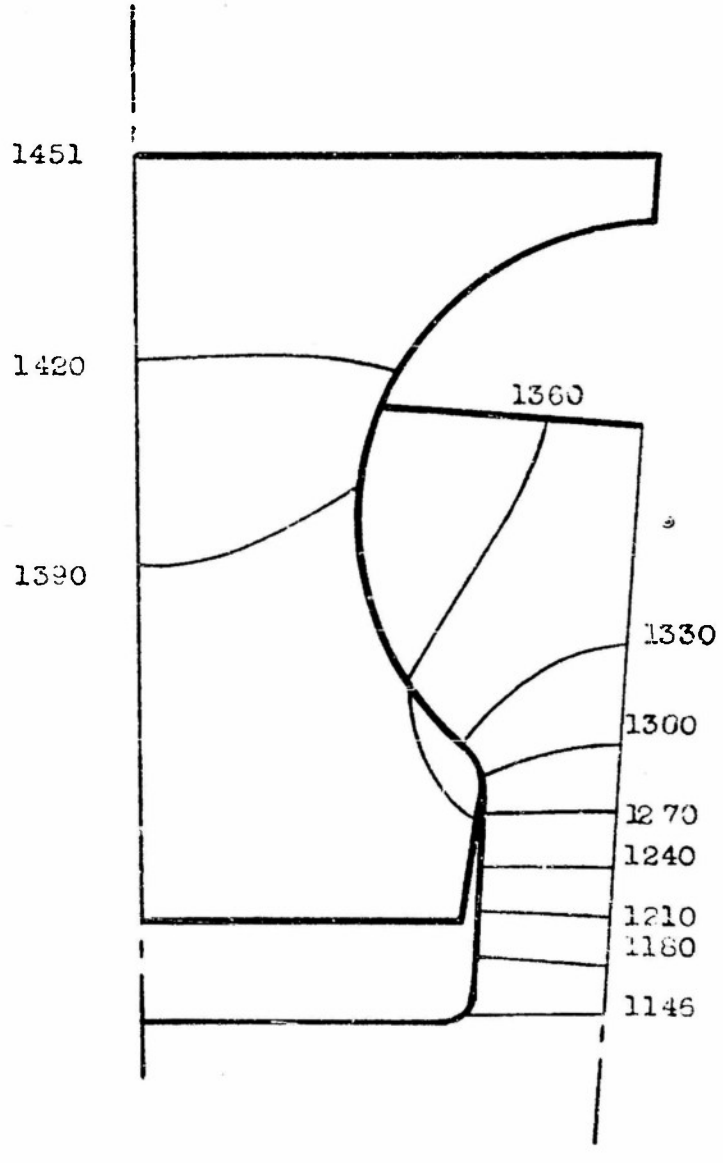

Figure 14: Temperature distribution through dovetail type attachment. Te = 1,600 °F , Q_o = 30, D_b/d_r = 2.7

Figure 15 Stress Rupture curves for cement materials

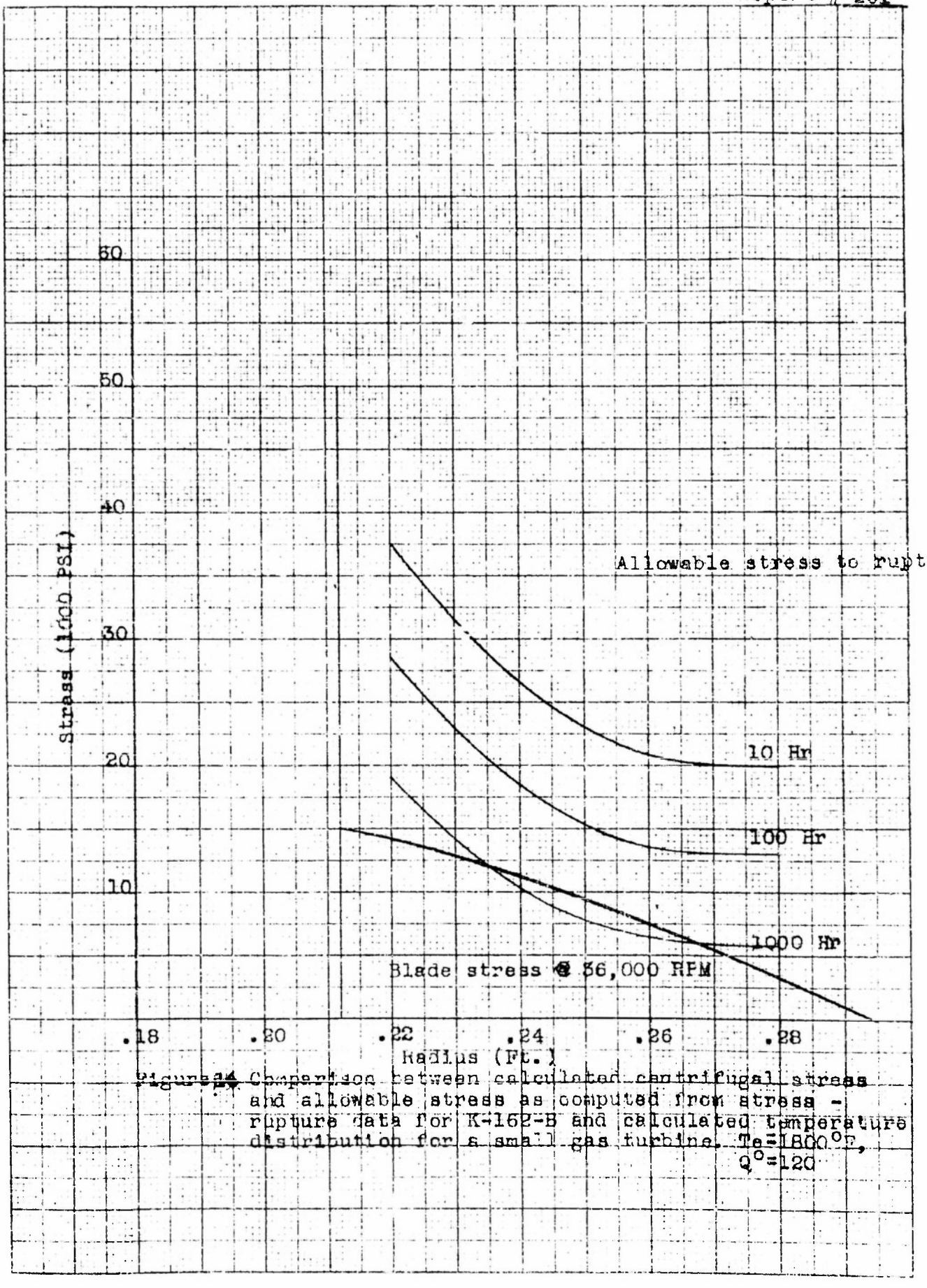

Figure 24 Comparison between calculated centrifugal stress and allowable stress as computed from stress - rupture data for K-162-B and calculated temperature distribution for a small gas turbine. T_e=1800°F, Q^o=120

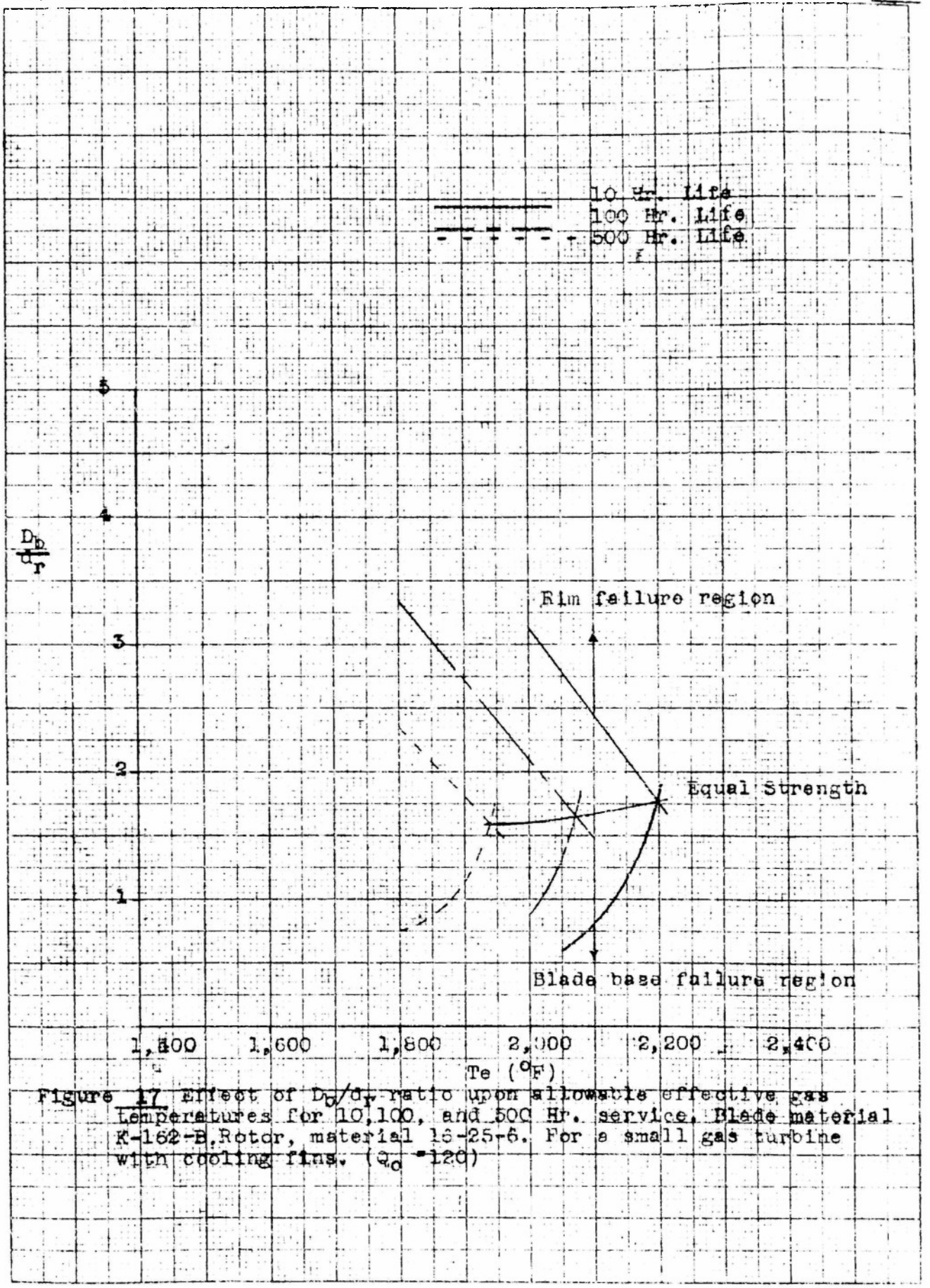

Figure 17 Effect of D_b/d_r ratio upon allowable effective gas temperatures for 10,100, and 500 Hr. service. Blade material K-162-B, Rotor, material 16-25-6. For a small gas turbine with cooling fins. (Q_o =120)

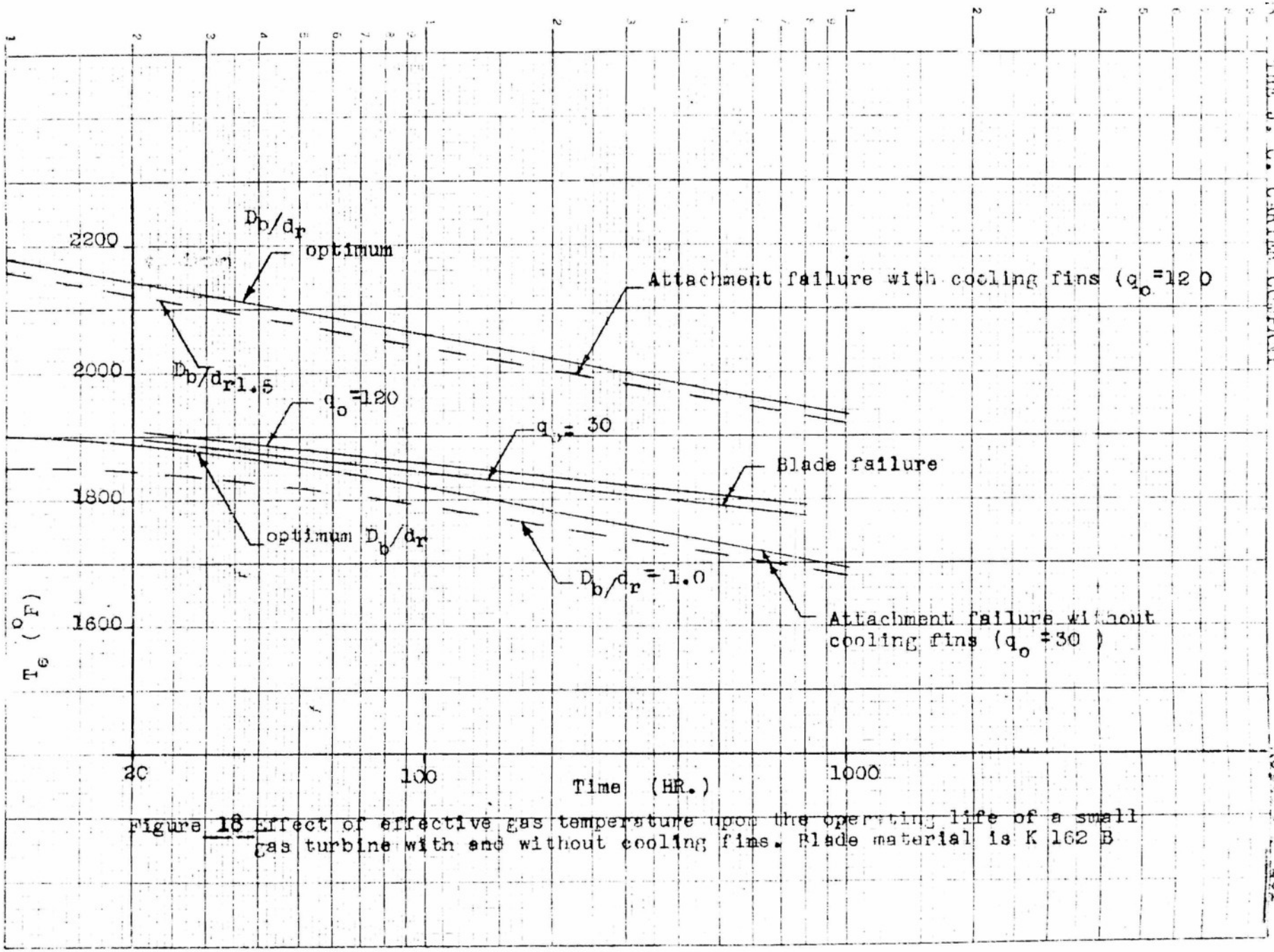

Figure 18 Effect of effective gas temperature upon the operating life of a small gas turbine with and without cooling fins. Blade material is K 162 B

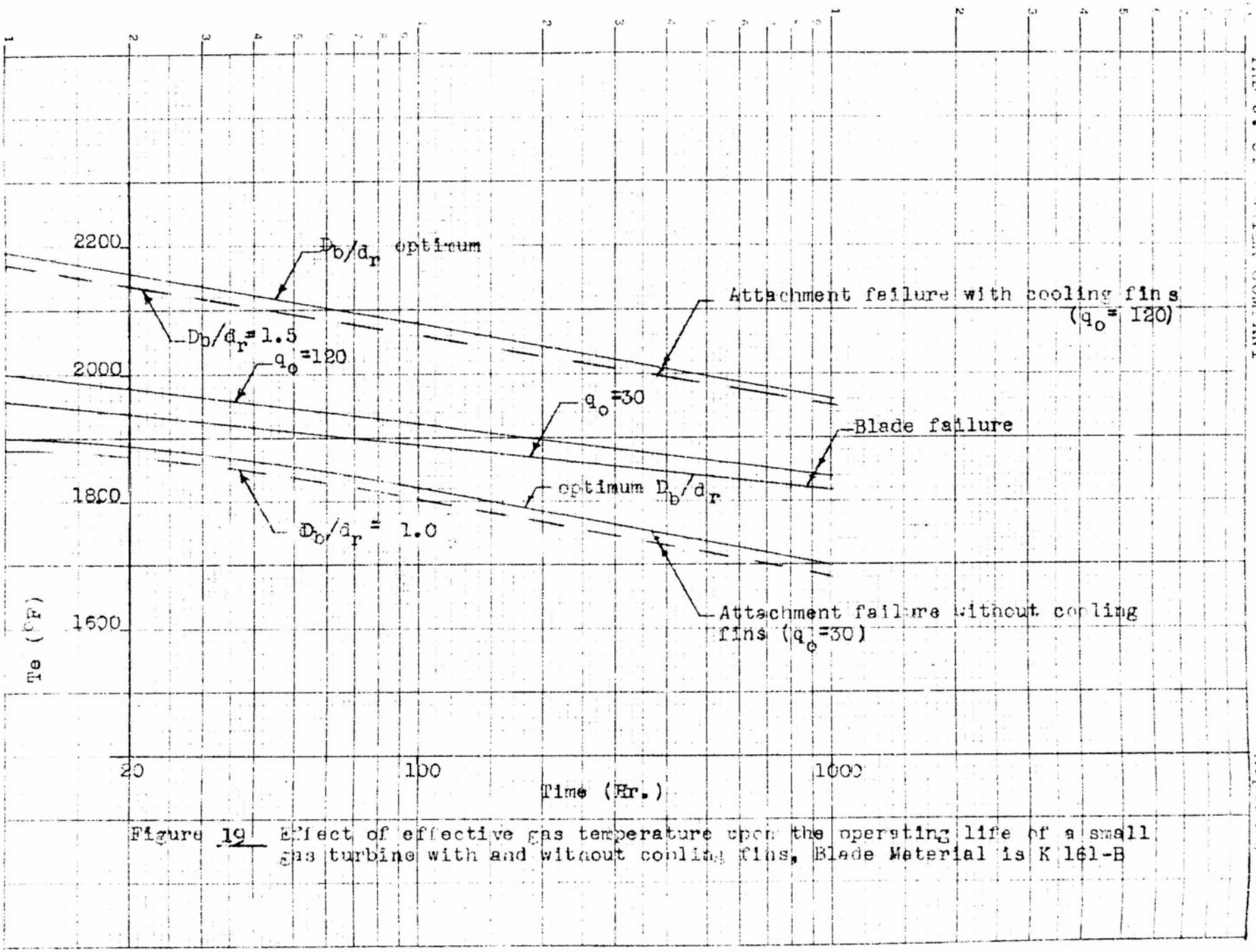

Figure 19 Effect of effective gas temperature upon the operating life of a small gas turbine with and without cooling fins. Blade Material is K 161-B

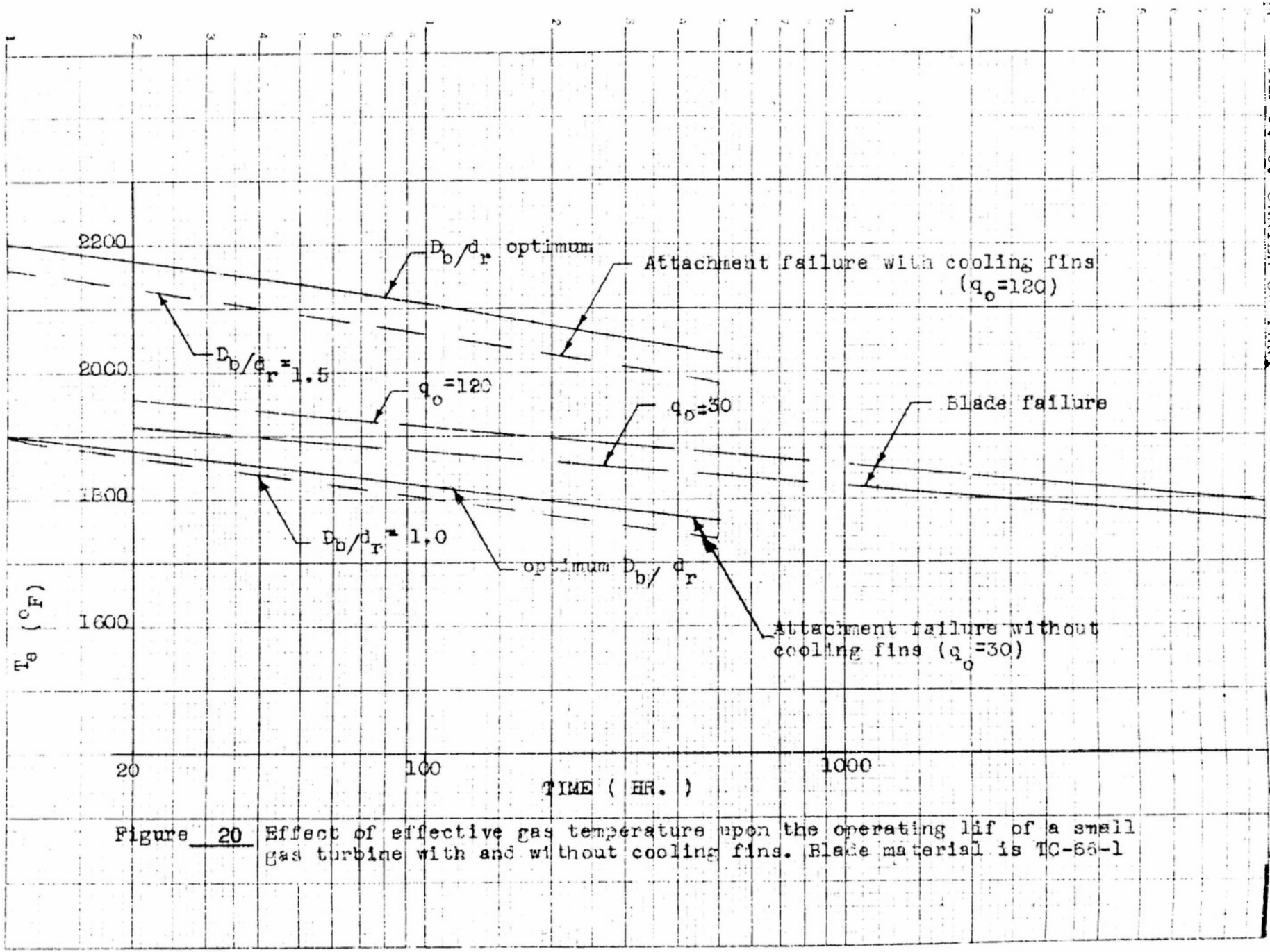

Figure 20 Effect of effective gas temperature upon the operating life of a small gas turbine with and without cooling fins. Blade material is TC-66-1

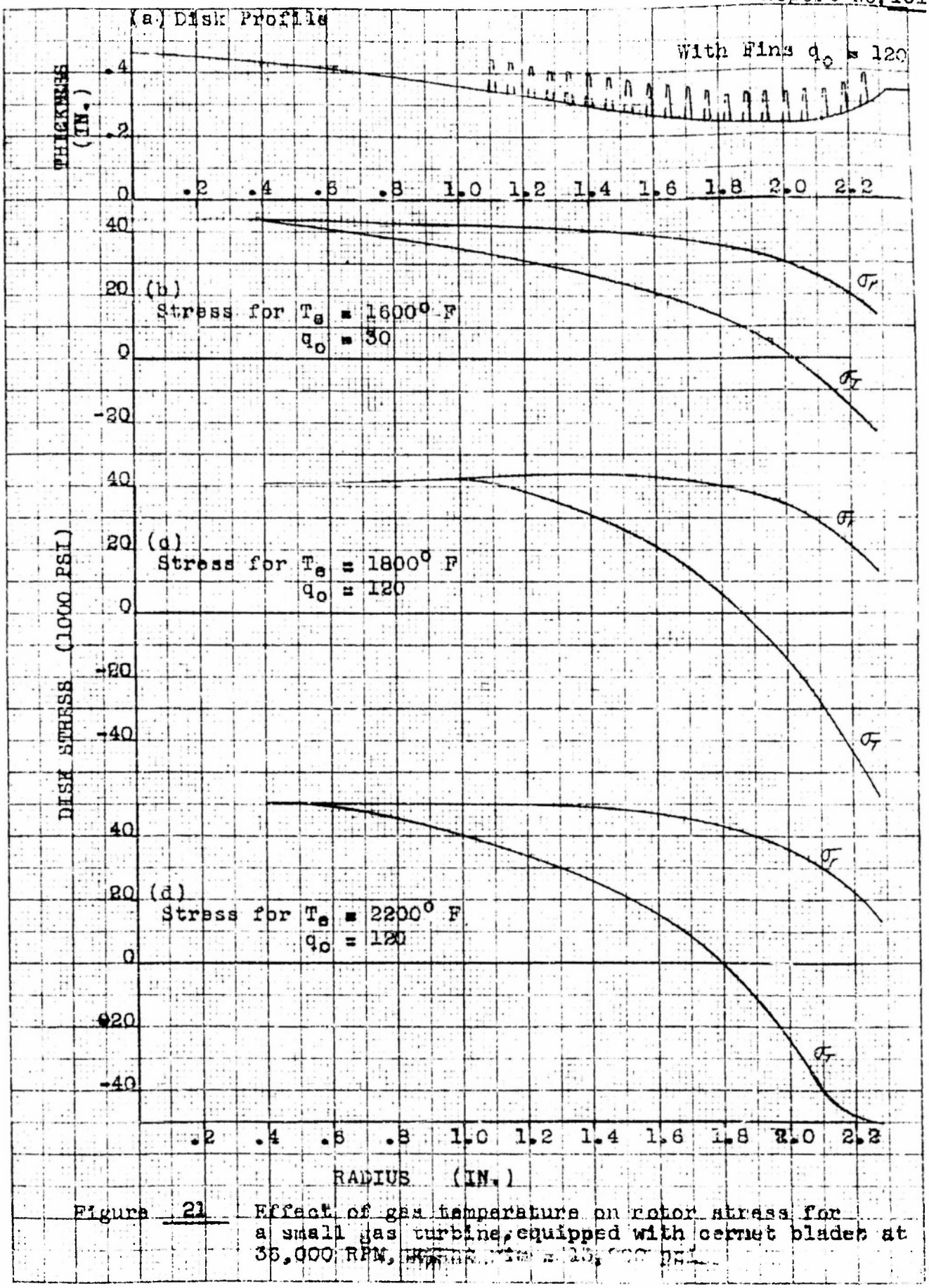

Figure 21 — Effect of gas temperature on rotor stress for a small gas turbine, equipped with cermet blades at 36,000 RPM, [illegible]

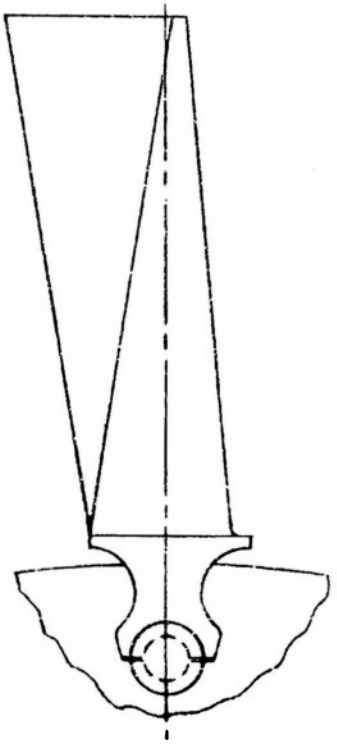

Rivet Retainer

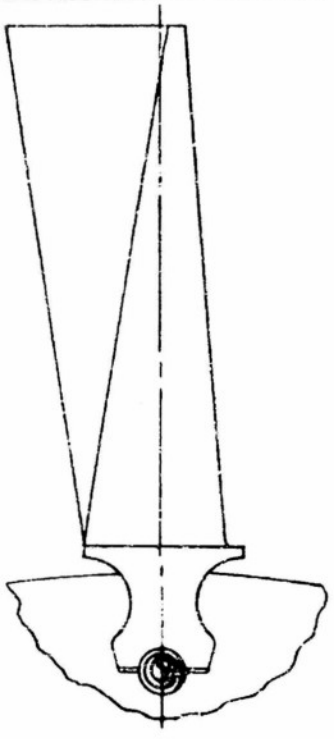

Self-locking Pin Retainer

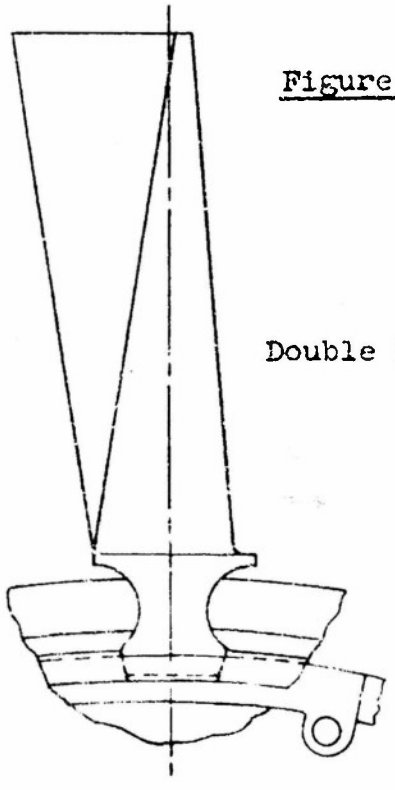

Double Snap-Ring Retainer

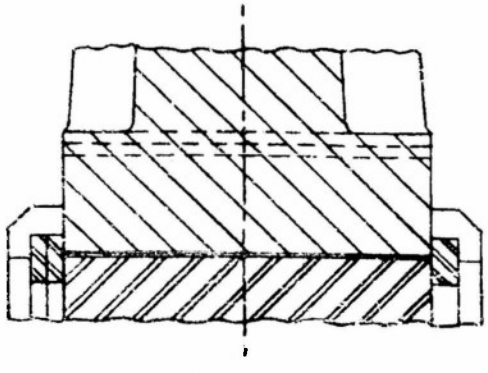

Figure 22 - Suggested blade retaining methods.